12-2007

Design of Multi-Electron Transfer Catalysts for the Reduction of Trichloroethylene

Christopher Gerard Eman Ciptadjaya

DESIGN OF MULTI-ELECTRON TRANSFER CATALYSTS FOR THE REDUCTION OF TRICHLOROETHYLENE

by

Christopher Gerard Eman Ciptadjaya

A Thesis
Submitted to the
Faculty of The Graduate College
in partial fulfillment of the
requirements for the
Degree of Master of Science
Department of Chemistry

Western Michigan University
Kalamazoo, Michigan
December 2007

ACKNOWLEDGMENTS

I would like to take this opportunity to thank my research advisor, Professor Sherine O. Obare, for all her guidance and support throughout my career as a graduate student at Western Michigan University. Her broad knowledge and passion for science has enabled me to develop as a scientist and I have learned a great deal of chemistry from her. She always encourages and motivates me to excel in my research and studies. I am deeply grateful for all her help, inside and outside of the lab. I would like to thank the Obare former and present group members who have always been there to support me throughout my graduate career.

I would also like to thank Dr. Yirong Mo and Dr. Subra Muralidharan for serving as members of my thesis committee and taking the time to review my work. I appreciate their guidance and help.

Last but not least, I would like to thank my parents, Peter Sanjaya and Nancy Tanudarma, who have always been there for me at all times, and have been truly supportive. I would also like to acknowledge my aunt, Jilly Sulyanto and her beloved family. I am extremely grateful for their tremendous support and love.

This research was supported by the National Science Foundation Faculty Early Career Development (CAREER) and Michigan Economic Development Corporation (MEDC) grants to Dr. Sherine O. Obare.

Christopher Gerard Eman Ciptadjaya

DESIGN OF MULTI-ELECTRON TRANSFER CATALYSTS FOR THE REDUCTION OF TRICHLOROETHYLENE

Christopher Gerard Eman Ciptadjaya, M.S.

Western Michigan University, 2007

For decades, organohalide (RX) compounds have been heavily used in the chemical and pharmaceutical industries and in agriculture as pesticides. Improper disposal of organohalides has resulted in their presence in the environment as pollutants, and they have therefore presented serious environmental and toxicological concerns. These organohalides have been associated with various health and environmental problems. Therefore, effective methods for their remediation are required. We have developed a multi-electron transfer (MET) catalyst consisting of flavin mononucleotide anchored to nanocrystalline mesoporous titanium dioxide (TiO_2) thin films, and examined its reactivity toward the organohalide pollutant trichloroethylene (TCE). Various environmental factors were used to control the reactivity of the catalytic system. The results indicated that the reactivity of reduced FMN increased significantly when anchored to nanocrystalline TiO_2. Spectroelectrochemical data suggested that the increased reactivity is due in part to a substantial negative shift in the FMN/$FMNH_2$ reduction potentials induced when FMN is anchored to the TiO_2 surface. The reactivity of the FMN/TiO_2 towards TCE was examined both in aqueous and methanol solvent.

TABLE OF CONTENTS

CHAPTER

Table of Contents—continued

CHAPTER

LIST OF TABLES

LIST OF FIGURES

CHAPTER I

THE NEED FOR NEW MATERIALS TO ADDRESS ENVIRONMENTAL REMEDIATION

1.1 Environmental Pollution

The civilian, commercial, and defense sectors of most advanced industrialized nations as well as developing nations are facing tremendous environmental concerns due to various contaminants. As a result of improper practices, air, water and soil are highly contaminated with various pollutants. This thesis addresses a class of water pollutants namely organohalides. Even though three-quarters of the earth's surface is water, only ~1% is available for drinking [3]. Water pollution occurs when waste, for example, oil, industrial acids, or farm pesticides, poisons aquatic plants and animals, enter the water system and cannot be removed or cleaned by natural processes. Most of these wastes can be highly toxic to various organisms as well as to human health. Water pollution arises from various sources including industrial waste, agricultural practices and various civilian practices [2]. Another form of water pollution is the clean but heated water discharged by power plants into waterways. This heated water, called thermal pollution, harms fish and aquatic plants by reducing the amount of oxygen in the water. Chemical and oil spills can also cause devastating water pollution that kills water birds, shellfish, and other wildlife.

Some water pollution occurs when there is improper separation of sewer wastewater from clean drinking water. In parts of the world that lack modern sewage

treatment plants, water carrying human waste can flow into drinking water supplies. Disease-carrying bacteria in the waste can then contaminate the drinking water and cause such illnesses as cholera and dysentery. In areas with good sanitation, most human waste flows through underground pipes to special treatment plants that kill the harmful bacteria and remove the solid waste.

According to the Eurochlor Organization, 80% of diseases are caused by contaminated drinking water supplies [3]. Some adverse health effects associated with drinking water contamination include damage to the central nervous system, the reproductive system, the liver, and the kidney. In addition, several forms of cancer have been linked to various water contaminants [7]. Therefore, it is important to maintain clean drinking water. In this regard, there is great interest amongst researchers to establish techniques and methodologies or to develop materials that are capable of degrading contaminants from the environment. The production and use of halogenated aliphatic compounds and their apparent hazards to human health have prompted investigations concerning their fate in the human body, in subsurface waters, and in treatment facilities. The productions of some common halogenated aliphatic compounds, their maximum contamination level and carcinogenetic effects are listed on Table 1.1.

Along with the various environmental contaminants that destroy our natural resources, drinking water tends to be highly affected, and much of taxpayers' money is spent ensuring the cleanliness of our drinking water supplies. The sustainability of drinking water is of serious concern [2-5]. The United States Environmental Protection Agency (EPA) consistently publishes lists of contaminants that must be regulated [2].

The database includes a total of 74 pesticides in 38 states, which require monitoring and regulation in ground water [6].

Table 1.1 Production, proposed maximum contaminant levels and toxicity ratings of common halogenated aliphatic compounds [8]

Compound	Production (million lb/yr)	MCL[b] (μg/L)	Carcinogenity[c]
Trihalomethanes	n/a	100	n/a
Vinyl chloride	7000	1	1
1,1-Dichloroethylene	200	7	3
trans-1,2-Dichloroethylene	<0.001	-	-
Trichloroethylene	200	5	3
Tetrachloroethylene	550	-	3
1,1-Dichloroethane	<0.001	-	-
1,2-Dichloroethane	12000	5	2
1,1,1,-Trichloroethane	600	200	3
1,2-Dibromoethane	332	-	3

[b] Maximum contaminant level

[c] Carcinogenity: 1 = carcinogenic; 2 = probably carcinogenic; 3 = unclassified

The US Environmental Protection Agency (EPA) has classified 6 types of common drinking water contaminants: (1) disinfectants (D), (2) disinfection byproduct (DBP), (3) microorganism (M), (4) organic chemical (OC), (5) inorganic chemical (IOC) and (6) radionuclide (R). Tabulation of national primary drinking water contaminants is listed in Table 1.2. Based on the compiled table, about 37.5% of the pollutants on the EPA's contaminants candidate list are organohalides [2].

Table 1.2 United States Environmental Protection Agency list of national primary drinking water contaminants [2]

Contaminant	Type	Contaminant	Type
Acrylamide	OC	Ethylbenzene	OC
Alachlor	OC	Ethylene dibromide	OC
Alpha particles	R	Fluoride	IOC
Antimony	IOC	Giardia lamblia	M
Arsenic	IOC	Glyphosate	OC
Asbestos (fibers > 10 micrometers	IOC	Haloacetic acids	DBP
Atrazine	OC	Heptachlor	OC
Barium	IOC	Heptachlor epoxide	OC
Benzene	OC	Heterotrophic plate count	M
Benzo(a)pyrene (PAHs)	OC	Hexachlorobenzene	OC
Beryllium	IOC	Hexachlorocyclopentadiene	OC
Beta particles and photon emitters	R	Lead	IOC
Bromate	DBP	Legionella	M
Cadmium	IOC	Lindane	OC
Carbofuran	OC	Mercury (inorganic)	IOC
Carbon tetrachloride	OC	Methoxychlor	OC
Chloramines (as Cl_2)	D	Nitrate (measured as Nitrogen)	IOC
Chlordane	OC	Nitrite (measured as Nitrogen)	IOC
Chlorine (as Cl_2)	D	Oxamyl (Vydate)	OC
Chlorine dioxide (as ClO_2)	D	Penthachlorophenol	OC
Chlorite	DBP	Picloram	OC
Chlorobenzene	OC	Polychlorinated biphenyls (PCBs)	OC
Chromium (total)	IOC	Radium 226 and Radium 228	R
Copper	IOC	Selenium	IOC
Cryptosporidium	M	Sumazine	OC
Cyanide (free)	IOC	Stryrene	OC
2,4-D	OC	Tetrachloroethylene	OC
Dalapon	OC	Thallium	IOC
1,2-Dibromo-3-chloropropane (DBCP)	OC	Toluene	OC
o-Dichlorobenzene	OC	Total Coliforms (fecal and E.coli)	M
p-Dichlorobenzene	OC	Total trihalomethanes	DBP
1,2-Dichloroethane	OC	Toxaphene	OC
1,2-Dichloroethylene	OC	2,4,5-TP (Silvex)	OC
cis-1,2-Dichloroethylene	OC	1,2,4-Trichlorobenzene	OC
trans-1,2-Dichloroethylene	OC	1,1,1-Trichloroethane	OC
Dichloromethane	OC	1,1,2-Trichloroethane	OC
1,2-Dichloropropane	OC	Trichloroethylene	OC
Di(2-ethylhexyl) adipate	OC	Turbidity	M
Di(2-ethylhexyl) phthalate	OC	Uranium	R
Dinoseb	OC	Vinyl Chloride	OC
Dioxin	OC	Viruses (enteric)	M
Diquat	OC	Xylenes (total)	OC
Endothall	OC		
Endrin	OC		
Epichlorohydrine	OC		

Ground water contamination is likely to be the primary source of human contact with toxic chemicals emanating from more than 70% of the hazardous waste sites in the United States. Classes of ground water contaminants include: solvents, volatile organics, chlorinated volatile organics, dioxins, dibenzofurans, pesticides, PCBs, chlorophenols, asbestos, heavy metals and arsenic compounds. Some specific compounds of interest are 4-chlorophenol, pentachlorophenol, trichloroethylene (TCE), perchloroethylene (PCE), CCl_4, $HCCl_3$, CH_2Cl_2, ethylene dibromide, vinyl chloride, ethylene dichloride, methyl chloroform, *p*-dichlorobenzene and hexachlorocyclopentadiene. The occurrence of TCE and PCE in soils and ground water is widespread.

1.2 Organohalide Pollutants

1.2.1 The Nature of Organohalide Compounds

Organohalide compounds (RX) are known to be highly toxic, carcinogenic and mutagenic even through exposure to minute concentrations. Organohalides exhibit a wide range of physical and chemical properties. These compounds consist of halogen-substituted hydrocarbon molecules, each of which contains at least one atom of F, Cl, Br or I. They may be saturated (alkyl halides), unsaturated (alkenyl halides), or aromatic (aryl halides) [9]. Common examples of low molecular mass RX compounds are shown in Figure 1.1.

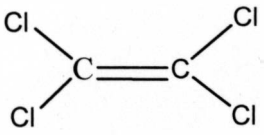

Tetrachloroethylene
(Perchloroethylene)

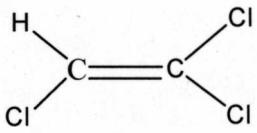

Trichloroethylene
(TCE)

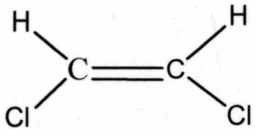

Cis-1,2-Dichloroethylene
(*Cis*-1,2-DCE)

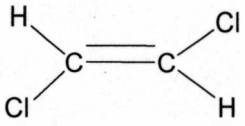

Trans-1,2-Dichloroethylene
(*Trans*-1,2-DCE)

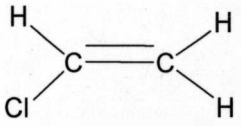

Vinyl chloride
(Monochloroethylene)

Figure 1.1 Structures of the common low-molecular-mass organohalides

These halogenated volatile organic compounds are widely used as industrial solvents, particularly for degreasing of metals and in the dry cleaning industry. The most widely manufactured organohalide compounds are chlorinated hydrocarbons, many of which are listed as hazardous substances and hazardous waste. Organohalides are common contaminants in gaseous emissions from industrial processes, landfills, hazardous waste sites, ground water remediation facilities and indoor air [9].

The introduction and usage of organohalides to the environment is inevitable due to their widespread use and applications in various pharmaceutical and chemical processes. It has been estimated that about 85% of all medicines either contain chlorine or use chlorine as part of the manufacturing processing [3]. In addition, organohalides are also commonly found in pesticides, such as dichloro-diphenyl-trichloroethane (DDT), adrin, heptachlor, and chlordane, which were banned in the 1970s because of their

persistence in the environment and toxicity to non-target species as well as humans. Drinking water acquired from sources such as underground aquifers are likely to be contaminated with various pollutants including organohalides [9]. Organohalide pollutants are present in wastewater and ground water and cause environmental contamination due to their impacts on human health [2, 5].

Organohalides are frequently found as contaminants in air, water, soil, food, and even in humans [10]. Due to their persistent nature, once they enter the environment they will stay and cause damage for decades. The half-lifes of a select group of organohalides are tabulated in Table 1-3. At ambient temperature, most of these organohalides tend to have a very long half-life. Vogel et al reported that CCl_4 has 7000 years half-life [8].

Organohalides are very inert in the environment. PCE and TCE have long environmental half-lifes due in part to their very slow oxidative breakdown under anaerobic conditions [8]. Organohalides are also widely distributed at the μg RX per 1 L of H_2O level in rainwater, water supplies, and ocean [11]. Concentrations of chlorinated hydrocarbons in the food chain have also been reported [12]. In 1975, 33 μg/L chloroform and 5 μg/L carbon tetrachloride were found in cheese.

Table 1.3 Half-lifes of halogenated compounds in aqueous solution at 20°C

Organohalides (RX)	Half-life (years)	Reference
Trichloroethylene	2	*Ground Water Monitoring and Remediation, 9, 129-140*
Chloroform	3500	*J. Phys. Chem. Ref. Data* 1978, *7*, 383-415
Carbontetrachloride	7000	*J. Phys. Chem. Ref. Data* 1978, *7*, 383-415
Trichloroethene	2.5	*Proc. R. Soc. London Ser. B.* 1975, *189*, 305-32
Tetrachloroethene	6	*Proc. R. Soc. London Ser. B.* 1975, *189*, 305-32

1.2.2 Trichloroethylene

Trichloroethylene (TCE) is one example of an organohalide that is found in many terrestrial and ground water environments. TCE is a nonflammable, colorless liquid with a somewhat sweet odor and a sweet, burning taste. It is used mainly as a solvent to remove grease from metal parts, but it is also an ingredient in adhesives, paint removers, typewriter correction fluids, and spot removers. Colorless, nonflammable liquid tetrachloroethylene (PCE) has properties and similar uses to those of trichloroethylene [9]. Just like tetrachloroethylene, trichloroethylene is not thought to occur naturally in the environment. However, it has been found in ground water sources and many surface waters as a result of the manufacture, use, and improper disposal of the chemicals.

Once trichloroethylene enters the environment, it can dissolve in a minute amount of water but it will remain in the ground water for a long time due to its persistent nature.

It can also evaporate from surface water where it is commonly found as vapor in the air. TCE evaporates less easily from the soil than from surface water, thus it might bind to particles and remain attached for a long time. If TCE binds to particles in water, it can eventually settle down at the bottom of the sediment.

Exposure to TCE can occur through a variety of routes such as through inhalation, ingestion or through skin penetration. Small amounts of TCE may cause headaches, lung irritation, dizziness, poor coordination and difficulty in concentration. Large amounts of TCE exposure can cause impaired heart function, unconsciousness, and can possibly lead to death. Prolonged exposure to TCE can result in nerve, kidney, and also liver damage. Drinking water contaminated with TCE may cause nausea, liver damage, unconsciousness and death. The National Toxicology Program (NTP) has classified TCE as a "reasonable anticipated human carcinogen" and The International Agency for Research on Cancer (IARC) has determined TCE as a "probable carcinogen to humans". The Occupational Safety and Health Administration (OSHA) have set the exposure limit to 100 parts of TCE per million parts of air (100 ppm) for an 8-hour work day, 40-hour work week. The EPA has set an a maximum contaminant level of TCE in drinking water at 0.005 mg/L or 5 parts of TCE per billion parts of water.

1.3 Environmental Remediation for Ground Water Contamination

Environmental remediation deals with the removal of pollution or contaminants from environmental media such as soil, ground water, sediments, or surface water. In

general, remediation is required for the general protection of human health, organisms, and the environment or from a brownfield site intended for redevelopment. The process of environmental remediation can be depicted by the utilization of a catalyst or a class of compounds that transform contaminated species into a benign species [13-16].

Remediation of organohalide (RX) pollutants is important for maintenance of underground aquifers and ground water resources. The removal and/or detoxification of various pollutants for the environment continues to represent a major challenge. Nonetheless, it is important to find efficient ways to decrease the high concentrations of organohalide pollutants effectively and efficiently without causing any side effects. Accordingly, the removal of organohalide contaminants either *in-situ* or by above ground treatment is an active research area. Many processes and technologies have been proposed over the years to clean up polluted water. The typical remediation schemes commonly involve pumping the contaminated ground water to the surface and passing it through treatment systems. During this process, the pollutants are either degraded (for example via advanced oxidation processes) or are transferred to other media (as in the case of air stripping and granular activated carbon) [17].

Chlorinated ethylenes are likely to be degraded via reduction processes. This is because the carbon in chlorinated ethylenes, for example in TCE is in an oxidized state due of the presence of the chlorine atoms. Chlorinated ethylenes such as PCE and TCE can also be reduced microbially under methanogenic, acetogenic, and sulfate-reducing conditions to dichloroethenes (mainly *cis*-1,2-DCE), vinyl chloride, ethene and ethane. Enzymes such as PCE reductase, which contain corrinoids, are responsible for catalyzing the process. [18] However, it is well-known that both DCE and vinyl chloride are more

toxic than TCE and PCE. Many microbial organisms can even use PCE and TCE as electron acceptors by reducing it them to *cis*-DCE. Therefore, materials that can avoid DCE formation from TCE or PCE are in demand.

1.4 Nanoscale Materials in Environmental Remediation

Advances in nanoscale science and engineering present novel opportunities to develop cost effective and environmentally acceptable solutions toward environmental remediation, including maintenance of water quality [4, 15, 19, 20]. Improving water quality is critical to sustained health. Figure 1.2 highlights four classes of nanoscale materials that are currently used for water purification. These include metal-containing nanoparticles, carbonaceous nanomaterials, zeolites, and dendrimers [4]. These materials are used because they have a broad range of physicochemical properties that make them particularly attractive as separation and reactive media for water purification.

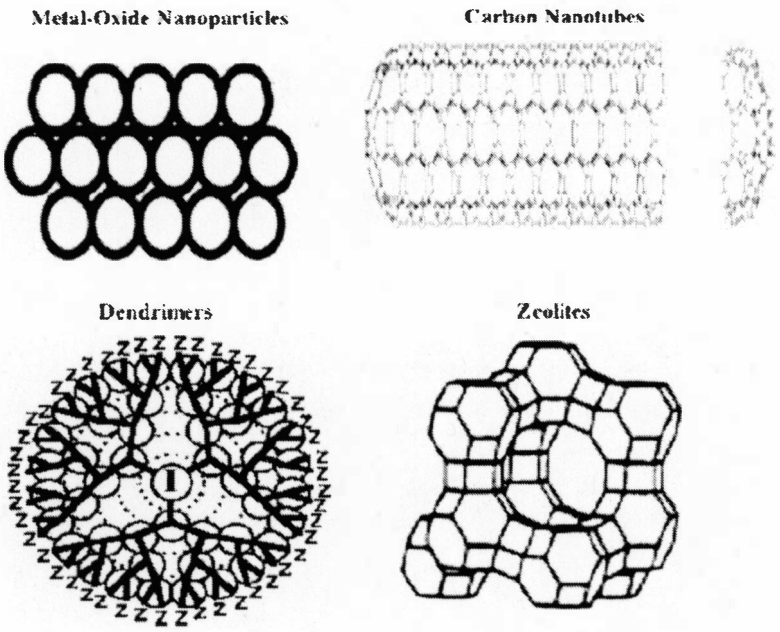

Figure 1.2 Various nanomaterials that are currently being used as functional materials for water purification

Nanoscale materials offer several advantages over their bulk counterparts for use in environmental remediation. For example, nanostructured materials have higher surface area-to-volume ratio that could lead to enhanced reactivity with environmental contaminants that degrade through inner-sphere (adsorption) mechanisms [21]. In addition, nanosized particles can display quantum size effects, wherein the band gap (the separation between the valence band maximum and the conduction band minimum) energy increases with the decrease in particle size [21]. Quantum confinement is typically observed when the particle size is <10 nm, and this is dependent on the nature of the material. In addition to increased surface area-to-volume ratio and quantum size effects, the properties of nanostructures can be tuned toward specific environmental remediation applications through surface modification. Surface modification involves the

modification of the nanoparticle surface with a second material to optimize the desired remediation process. The advantages of surface modification are as follows: 1) The photoresponse of wide band gap semiconductors can be extended to the visible by coupling to another semiconductor or by covalently linking to a dye molecule. 2) Conduction band electrons in the semiconductor can be used to maintain a desired redox state of environmental catalysts and 3) increasing the stability of materials and enhancing its reactivity.

Technological advances in environmental sciences require new catalysts that effectively degrade organohalides (RX)s. Two classes of nanomaterials have gained considerable interest for environmental remediation: (1) zero-valent iron and (2) photocatalytic titanium dioxide. Reports using metals, or photocatalysts consisting of titanium dioxide have been shown to be relatively effective [16, 22, 23]. In the case of photocatalysis, there is clear evidence that direct photolysis also leads to degradation of the organohalides (RX), and thus the technique leads to a large distribution of products [42].

1.4.1 Zero-Valent Iron (Fe^0) Technology

The use of zero-valent metals to degrade contaminants represents an active area of research. This research was pioneered by Gillham and co-workers whereby Fe^0 was used as an immobilized reagent in a passive approach to ground water remediation. Iron's utility in subsurface treatment walls for removing organohalides has been confirmed by

controlled field experiments [17]. Zero-valent iron (Fe^0) has been studied extensively for organohalide remediation in ground water [16, 24-27]. In the environment, iron acts as an electron donor and reduces RX pollutants. For example, Pearson et. al., reported methylamine as a product of the reactions of halonitromethanes with Fe^0 [28].

Since Fe^0 does not exist naturally in the environment, it is a challenge to maintain the reactive redox state at the iron surface. In addition, the Fe^0 catalysts can generate products that are more toxic than the parent compound. For example, the reaction of iron powders with highly chlorinated hydrocarbons such as tetrachloroethylene (PCE) and trichloroethylene (TCE) produces *cis*-1,2-dichloroethene (DCE) and vinyl chloride (VC) [17, 29]. The rates and pathways of TCE dechlorination by iron fillings have been intensively studied and well understood. In the reaction between TCE and iron fillings, TCE is reduced and releases chloride ions, while iron is oxidized [17, 29].The proposed reaction pathways are β-elimination (primary), hydrogenolysis (minor) and hydrogenation (minor). These mechanisms explain the formation of ethene and ethane as the main products, with minor amounts of chlorinated intermediates (formed via hydrogenolysis) and acetylene (formed via β-elimination) [25, 30]. According to the U.S. Environmental Protection Agency, the drinking water limit for vinyl chloride is 0.002 mg/L, which when compared to TCE (0.005 mg/L), indicating the increased toxicity of vinyl chloride relative to TCE.. In addition to increased toxicity, both *cis*-1,2-dichloroethylene as well as vinyl chloride react relatively slowly with Fe^0 [17].

Zhang et al. reported that iron particles are more reactive when coated with another metallic particle because the supporting metals prevent oxidation of the reactive iron surface sites [16, 31, 32] They found that the reactions of TCE with Pd/Fe

nanoparticles is ~7 times faster compared to Fe nanoparticles under the same conditions [32]. In addition, the products of the reactions yielded no toxic products such as DCE and VC. In most Fe^0 reactions with organohalide pollutants, inner sphere surface mediated electron transfer processes have been proposed [29].

Mallouk and coworkers also reported the effective dehalogenation of trichloroethylene (TCE) using a high-surface area nickel-iron nanoparticles [33]. The final TCE degradation products formed are even-numbered saturated hydrocarbons, such as butane, hexane and octane and trace amounts of toxic products such as vinyl chloride, 1,1-dichloroethylene, *cis*-1,2-dichloroethylene and *trans*-dichloroethylene [33].

Even though Fe^0 has been extensively used, there are a few difficulties associated with the Fe^0 technology. In addition to the low reactivity of iron powders with highly chlorinated hydrocarbons such as tetrachloroethylene (PCE) and trichloroethylene (TCE), research has shown a decrease in iron reactivity over time [31] and furthermore, there are engineering difficulties in the construction of metal walls in aquifers deeper than 30 m [31].

1.4.2 Remediation using Photocatalysis by TiO_2

During the last decade, titanium dioxide nanoparticles have emerged as promising photocatalysts for water purification. Heterogeneous TiO_2 photocatalysis is a growing area of research because of its capability in degrading many organic pollutants [14, 19, 34-36]. For instance, Yamazaki-Nishida et al reported gas-phase TCE photodegradation

to CO_2 and HCl in a packed-bed reactor containing highly porous TiO_2 pellets [23]. In general, anatase has long been considered as the most photochemically active phase of TiO_2, probably because of a higher surface adsorptive capacity towards many organic compounds, while rutile phase is generally less active because of higher rates of recombination of the photogenerated charge carriers [21].

Some potential advantages of nanostructured semiconductor materials for detoxification of organohalides include: 1) an enormous surface area for pollutant or catalyst activation, 2) redox and optical properties that can often be systematically tuned with particle size and/or shape [37, 38] and 3) surfaces that are easily functionalized for enhanced reactivity with organohalide pollutants [21, 39]. A disadvantage of TiO_2 is that ultraviolet irradiation is required. TiO_2 semiconductor has been studied extensively for oxidative and reductive remediation of organic contaminants in aqueous solution. The conduction band electrons produced by photolysis react with variety of organohalides (PCBs, halogenated alkanes, pesticides) through a reductive dehalogenation process. A proposed reductive dehalogenation pathways mechanism that could be initiated by band gap illumination of TiO_2 is shown in equations below 1a-c [40, 41].

$$TiO_2 + \text{solar light} \rightarrow TiO_2 (h^+_{VB} + e^-_{CB}) \qquad \text{(Eq. 1a)}$$

$$RX + TiO_2(e^-) \rightarrow R\bullet + X^- \qquad \text{(Eq. 1b)}$$

$$\text{Or} \quad RX + 2\ TiO_2(e^-) \rightarrow R^- + X^- \qquad \text{(Eq. 1c)}$$

Photoreactive degradation of organohalide pollutants may occur by either one- or multi-electron transfer processes. Choi and Hoffmann observed reaction products after

the photoreduction of TiO_2 in the presence of CCl_4 that strongly suggested both one- and two-electron transfer intermediates were present [42]. Based on the observation, it was concluded that two-electron transfer reduction of CCl_4 was thermodynamically favorable compared to one electron transfer pathway.

1.5 Electron Transfer for Environmental Remediation

1.5.1 Inner- and Outer-Sphere Electron Transfer

Since the late 1940s, the field of electron transfer processes has grown enormously, both in chemistry and biology. The mechanism of electron transfer was first elucidated by Rudolph A. Marcus in 1956 to address an outer-sphere electron transfer. The Marcus theory of electron transfer was then extended to include an inner-sphere electron transfer by the work of Noel Hush. The combined theory, called the Marcus-Hush theory, has given guidance to most electron transfer reactions. The classical studies by the late Henry Taube established that redox reactions in fluid solution occur by two different mechanisms: inner- and outer-sphere. In an outer sphere mechanism, the coordination sphere of the electron donor and acceptor remain constant throughout the redox reaction. In other words, an electron is transferred from one primary bond system to another. In an inner sphere mechanism, a ligand bridges the donor and the acceptor during the electron transfer event and electron transfer occurs within a primary bond system [43].

The redox reaction of RX has been proposed to occur via inner sphere mechanisms using $Cr(H_2O)_6^{2+}$ and an iron(II) porphyrin (iron meso-tetra(4-carboxyphenyl)porphyrin chloride, Fe(II) TCP). Both of these reductants react with organohalides by dissociative inner sphere single-electron transfer [44]. Evidence for inner-sphere electron transfer has been provided by observation of metal-carbenes in the reductions of CCl_4 and DDT. UV-visible spectral studies of inner-sphere electron transfer of heme catalysts with CCl_4 and DDT and the formation of carbene adducts have been established in the past 30 years [45, 46]. In 1997, Mansuy et al. demonstrated formation of carbene products in the reactions of iron porphyrins and DDT in the presence of Fe^0 or other reductants [46]. This produces evidence for an inner-sphere electron transfer mechanism. However, one cannot rule out the possibility that the carbene is formed by an outer-sphere mechanism which then coordinates to the iron center.

On the contrary, some research group also suggests that the reduction of RX is an outer-sphere electron transfer mechanism [47-49]. The most clear evidence of outer-sphere electron transfer was provided by McNeill et al where they utilized outer-sphere electron transfer agents composed of both aromatic radical anions and cobaltocenes to reduce TCE [47]. The aromatic radical anions utilized as reducing agents were naphthalene, pyrene, perylene because they offer a range of reduction potentials with well-studied behavior. The second class of reducing agents, decamethylcobaltocene and cobaltocene was chosen because the agents are well-characterized cobalt-centered reductants and because of the similarity of cobaltocene's reduction potential to that of the vitamin B_{12} Co^{I}/Co^{II} couple ($E_{1/2}$ = -0.58 V). In all cases, the same four products were observed: cDCE, tDCE, dichloroacetylene, and chloroacetylene. It was observed that the

outer-sphere reduction of TCE leads to [cDCE]:[tDCE] ratios of less than 5:1 and thus provides a basis for use of this product ratio as a diagnostic for the mechanism of TCE reduction.

1.5.2 Multi-Electron Transfer Systems for Environmental Remediation

Multi-electron transfer reduction of organohalide pollutants is a promising area of research [13, 25, 39, 50, 51]. It has theoretically been predicted that two-electron transfer reduction potentials of many organohalide pollutants are more positive than the one-electron transfer reduction potentials [51]. Two electron transfers pathways can occur at potentials where competitive O_2 or proton reductions are minimal.

Totten et al calculated the reduction potentials of various chlorinated ethylenes in aqueous solution at 20 °C as shown in Table 1.3. [51] The reduction potentials were measured against a standard hydrogen electrode (SHE). Based on the calculations, two-electron reduction potentials were found to be more positive compared to one-electron reduction potentials. This indicates that the reduction of chlorinated ethylenes with two electrons is more thermodynamically favored compared to one-electron reduction. As a result, reduction of organohalides occurs easier with systems that provide two-electrons.

Table 1.3 Calculated one- and two-electrons reduction potentials for reduction of chlorinated ethylenes in water [51]

Chlorinated Ethenes	One-electron reduction potential (E°_1) vs. SHE (Volt)	Two-electrons reduction potential (E°_2) vs. SHE (Volt)
CH_2=CHCl	-1.141	+ 0.386
ClCH=CHCl	-1.012	+ 0.464
H_2C=CCl_2	-0.802	+ 0.497
ClCH=CCl_2 (*)	-0.674	+ 0.537
Cl_2C=CCl_2	-0.598	+ 0.598

* The one- and two-electron reduction potentials are dependent on the products formed. The values given are for *cis*-dichloroethylene radical, •CCl=CHCl (one-electron reduction) and *cis*-dichloroethylene, ClHC=CHCl (two-electron reduction).

1.6 Research Objectives and Hypothesis

The main objectives of this research are to:

1. Establish a catalyst system that reacts with chlorinated ethylenes via two-electron transfer
2. Develop a catalyst system that promotes chlorinated ethylenes degradation in aqueous solution. (Aqueous-phase catalysis is desirable because it mimics real environmental conditions).
3. Compare reduction rate constants of one-electron transfer catalysts and two-electron transfer catalysts for chlorinated ethylenes

We investigated the effects of organic-inorganic hybrid catalysts toward the reduction of the organohalides (RX), in particular trichloroethylene (TCE). We observed a notably high reactivity between the catalysts and the organohalides (RX). Here, we report a new hybrid catalyst consisting of riboflavin 5'-mononucleotide (FMN) anchored to nanocrystalline titanium dioxide (TiO_2) particles assembled as depicted in Figure 1.3 Because FMN can be reduced to $FMNH_2$ thus carrying two electrons and TiO_2 photoreduction under appropriate conditions leads to electrons being trapped in the TiO_2 conduction band, the system can be modulated to have multiple electrons. Systems that deliver multiple electrons to a substrate for example an organohalides (RX) are advantages because they allow reactions to be carried out under mild conditions.

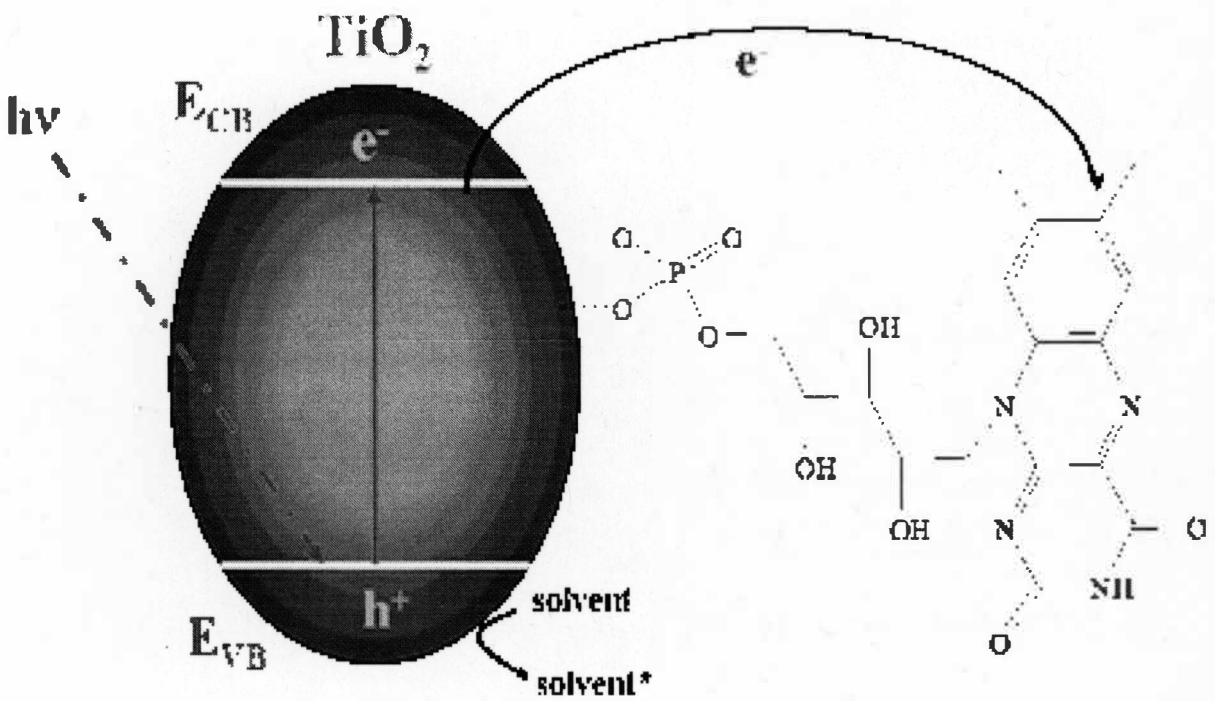

Figure 1.3 Schematic representation of electron transfer from TiO_2 to FMN following electron-hole charge separation

1.7 Conclusions

Nanoparticles offer great potential as water-purification catalysts and redox active media due to their large surface areas, their sizes and shape-dependent optical, electronic, and catalytic properties. Nanomaterials will become critical components of industrial and public water purification systems as more cost-effective and environmentally friendly nanomaterials are synthesized.

Current remediation techniques for organohalides including zero-valent iron technologies and visible-light activated TiO_2 nanoparticles have provided significant impact toward ground water remediation. However, there are some limitations associated with the application of zero-valent iron on ground water remediation, such as high cost, lack of flexibility, and the toxicity of the byproduct. The mechanism of electron transfer for RX reduction has been proposed through the inner-sphere and outer-sphere electron transfer.

The development of a catalyst that can react with RX via a two-electron and multi-electron transfer reaction is desirable compared to just a single-electron transfer reaction. Organic-inorganic hybrid catalyst composed of FMN/TiO_2 has been proposed to be a system that can store, trap, transfer, and deliver multiple electrons for RX remediation.

The integration of nanostructured materials in environmental science is a promising and exciting area of current and future research. Even though there is still many fundamental and mechanistic details that need to be elucidated for practical applications, it is clear that nanomaterials will contribute to solve major environmental problems.

1.8 References

1. *World Health Organization.* Water, Sanitation and Health [cited 2007; Available from: http://www.who.int/water_sanitation_health/en/.

2. US Environmental and Protection Agency[cited 2007; U.S. Environmental Protection Agency]. Available from: www.epa.gov/safewater/gwr/gwrprop.pdf.

3. Eurochlor [cited August 2007; Eurochlor Organization]. Available from: www.eurochlor.org.

4. Savage, N. and M.S. Diallo, Nanomaterials and water purification: Opportunities and challenges. Journal of Nanoparticle Research, **2005**. *7*: p. 331.

5. Simmons, J.E., Richardson, S.D., Rice, G., Hunter, E.S., and Tueschler, L.K, Development of a research strategy for integrated technology-based toxicological and chemical evolution of complex mixtures of drinking water disinfection byproducts. Environmental Health Prespectives, **2002**. *110*: p. 1013-1024.

6. Goodrich, J.A., B.W. Lykins, and R.M. Clark, Drinking water from agriculturally contaminated ground water. Journal of Environmental Quality, **1991**. *20(4):* p. 707-717.

7. Ruder, A.M., Potential Health Effects of Occupational Chlorinated Solvent Exposure. Annual New York Academic Science, **2006**. *1076*: p. 207-227.

8. Vogel, T.M., C.S. Criddle, and P.L. McCarty, Transformations of halogenated aliphatic compounds. Environment and Science Technology, **1987.** *21*: p. 722-736.

9. Manahan, S.E., Hazardous Waste Chemistry, Toxicology and Treatment. **1990**, CRC Press.

10. Chester, G., Levy, J., Fathulla, R.N., and Harkin, J.M., Environmental fate of alachlor and metalochlor. Review on. Environmental Contamination Toxicology, **1989**. *110*: p. 1-74.

11. Pearson, C.R., Chlorinated C1 and C2 hydrocarbons in the marine environment. Proceeding Royal Society of London. B., **1975.** *189*: p. 305-332.

12. McConnell, G., D.M. Ferguson, and C.R. Pearson, Chlorinated hydrocarbons and the environment. Endeavour, **1975**. *34:* p. 13-18.

13. Obare, S.O., T. Ito, and G.J. Meyer, Controlling Reduction Potentials of Semiconductor-Supported Molecular Catalysts for Environmental Remediation of Organohalide Pollutants. Environmental Science and Technology, **2005**. *39*: p. 6266-6272.

14. Canevali, C., Morazzoni, F., Scotti, R., Giusti, M., Testino, A., Musinu, A., and Cannas, C., Nanocrystalline TiO_2 with Enhanced Photoinduced Charge Separation as Catalyst for the Phenol Degradation. International Journal of Photoenergy, **2006**. *90809*: p. 1-6.

15. Ranjit, K.T., Medina, G., Jeevanandam, P., Martyanov, I.N., Klabunde, K.J., Nanoparticles in environmental remediation. Environmental Catalysis, ed. V.H. Grassian. **2005**, Boca Raton, Fla: CRC Press LLC. 391-420.

16. Zhang, W.X., Nanoscale iron particles for environmental remediation: An overview. Journal of Nanoparticle Research, **2003**. *5*. p. 323-332.

17. W. Scott Orth, and R.W. Gillham., Dechlorination of Trichloroethene in Aqueous Solution Using Fe^0. Environmental Science and Technology, **1996**. *30(1):* p. 66.

18. Glod, G., Angst, W., Holliger, C., and Schwarzenbach., R.P.., Corrinoid-Mediated Reduction of Tetrachloroethylene, Trichloroethylene, and Trichlorofluoroethene in Homogeneous Aqueous Solution: Reaction Kinetics and Reaction Mechanisms. Environmental Science and Technology, **1997**. *31*: p. 253-260.

19. Prairie, M.R., Evans, L.R., Stange, B.M., and Martinez, S.L., An investigation of TiO_2 Photocatalysis for the Treatment of Water Contaminated with Metals and Organic Chemicals. Environmental Science and Technology, **1993.** *27*: p. 1776-1782.

20. Duran, N. and E. Esposite, Potential applications of oxidative enzymes and phenoloxidase-like compounds in wastewater and soil treatment. Applied Catalysis B: Environmental, **2000**. 28: p. 83-99.

21. Obare, S.O. and G.J. Meyer, Nanostructured materials for environmental remediation of organic contaminants in water. Journal of Environmental Science and Health A, **2004**. *39(10):* p. 2549-2573.

22. Chen, X. and S.S. Mao, Titanium Dioxide Nanomaterials: Synthesis, Properties, Modifications and Applications. Chemical Reviews, **2007**.107(7): p. 2891-2959.

23. Yamazaki-Nishida, S., Nagano, K.J., Phillips, L.A., Cevera-March, S., and Anderson, M.A., Photocatalytic degradation of trichloroethylene in the gas phase using titanium dioxide pellets. Journal of Photochemistry and Photobiology A: Chemistry, **1993**. *70(1):* p. 95-99.

24. Matheson, M.J. and P.G. Tratnyek, Reductive Dehalogenation of Chlorinated Methanes by Iron Metal. Environmental Science and Technology, **1994**. *28*: p. 2045-2053.

25. Roberts, A.L., Totten, L.A., Arnold, W.A., Burns, D.R., and Campbell, T.J., Reductive Elimination of Chlorinated Ethylenes by Zero-Valent Metals. Environmental Science and Technology, **1996**. *30(8):* p. 2654-2659.

26. Vikesland, P.J., McGuire, M.M., Langley, L.A., Roberts, A.L., and Fairbrother, D.H., Applications of surface analysis in the environmental sciences: dehalogenation of chlorocarbons with zero-valent iron and iron-containing mineral surfaces. Analytica Chimica Acta, **2003**. *496*: p. 301-313.

27. Lien, H.L. and W.X. Zhang, Nanoscale iron particle for complete reduction of chlorinated ethenes. Colloids and Surfaces A: Physiochemical and Engineering Aspects, **2001**. *191*: p. 97-105.

28. Pearson, C.R., R.M. Hozalski, and W.A. Arnold, Degradation of chloropicrin in the presence of zero-valent iron. Environmental Toxicology and Chemistry, **2005**. *24*: p. 3037-3042.

29. Gillham, R.W. and O' Hannesin,al S.F., Enhanced degradation of halogenated aliphatics by zero-valent iron. Ground Water, **1994**. *32:* p. 958-967.

30. Orth, W.S. and R.W. Gillham, Dechlorination of trichloroethene in aqueous solution using Fe0. Environmental Science and Technology, **1996**. *30*: p. 66-71.

31. Wang, C.B. and W.X. Zhang, Synthesizing nanoscale iron particles for rapid and complete dechlorination of TCE and PCBs. Environmental Science and Technology, **1997**. *31*: p. 2154-2156.

32. Zhang, W., C.B. Wang, and H.L. Tien, Treatment of chlorinated organic contaminants with nanoscale bimetallic particles. Catalysis Today, **1998**. *40*: p. 387-395.

33. Schrick, B., Blough, J.L., Jones, D., and Mallouk, T.E., Hydrodechlorination of Trichloroethylene to Hydrocarbons Using Bimetallic Nickel-Iron Nanoparticles. Chemistry of Materials, **2002**. *14:* p. 5140-5147.

34. Anpo, M., Utilization of TiO_2 photocatalysts in green chemistry. Pure and Applied Chemistry, **2000**. *72(7):* p. 1265-1270.

35. Alberici, R.M., Mendes, A.M., Jardim, W.F., and Eberlin, M.E., Mass Spectrometry On-Line Monitoring and MS2 Product Characterization of TiO_2/UV

Photocatalytic Degradation of Chlorinated Volatile Organic Compounds. Journal of the American Society of Mass Spectrometry, **1998.** *9*: p. 1321-1327.

36. Park, J., Choi, E., Cho, I., and Kim, Y.G., Solar Light Induced Degradation of Trichloroethylene using TiO_2: Effects of Solar Light Intensity and Seasonal Variations. Journal of Environmental Science and Health, **2003.** *38(9):* p. 1915-1926.

37. Alivisibleatos, A.P., Prespective on the physical chemistry of semiconductor nanocrystals. Journal of Physical Chemistry, **1996**. *100*: p. 13226-13329.

38. Zhang, J.Z., Ultrafast studies of electron dynamics in semiconductor and metal colloidal nanoparticles: effects of size and surface. Accounts of Chemical Research, **1997**. *30*: p. 423-429.

39. Obare, S.O., Ito, T., Balfour, M., and Meyer, G.J., Ferrous Hemin Oxidation by Organic Halides at Nanocrystalline TiO_2 Interfaces. Nano Letters, **2003**. *3(8):* p. 1151-1153.

40. Radlowski, C. and W.V. Sherman, The gamma radiolysis of 2-propanol oxidation by carbon tetrachloride. Journal of Physical Chemistry, **1970**. *74*: p. 3043-3047.

41. Sherman, W.V., Evans, R., Nesyto, E., and Radlowski, C., Mechanism of the radiation-induced dechlorination of 1,1,1-trichloro-2,20-bis(p-chlorophenyl)ethane in alcoholic solution. Journal of Physical Chemistry, **1971**. *75*: p. 2762-2765.

42. Choi, W., Hong, S.J., Chang, Y.S., and Cho, Y., Photocatalytic degradation of polychlorinated dibenzo-p-dioxins on TiO_2 film under UV or solar light irradiation. Environmental Science and Technology, **2000.** *34*: p. 4810-4815.

43. Bard, A.J. and L.R. Faulkner, Electrochemical Methods: Fundamentals and Applications. 2nd ed, ed. D. Harris. 2001, New York: John Wiley and Sons,Inc.

44. Roberts, A.L., W.A. Arnold, and T. Kohn, Reactivity of substituted benzotrichlorides toward granular iron, Cr(II), and an iron(II) porphyrin: A correlation analysis. Environmental Science and Technology, **2006**. *40(13*): p. 4253-60.

45. Mansuy, D., M. Lange, and J.C. Chottard, Reaction of 2,2-bis(p-chlorophenyl)-1,1,1-trichloroethane (DDT) with iron (II) porphyrins. Isolation of the vinylidene carbene complex, tetraphenylporphyriniron (II). Journal of American Chemical Society, **1978**. *100*: p. 3213-3214.

46. Mansuy, D., M. Lange, and J.C. Chottard, Reaction of carbon tetrachloride with 5,10,15,20-tetraphenyl-porphinato iron (II): evidence for the formation of the carbene complex, Chemical Communication, **1977**. *18*: p. 648-649.

47. Follett, A.D. and K. McNeill, Reduction of Trichloroethylene by Outer-Sphere Electron-Transfer Agent. Journal of American Chemical Society, **2004**. *127*: p. 844-845.

48. Bonesi, S.M. and R. Erra-Balsells, Outer-sphere electron transfer from carbazoles to halomethanes. Reduction potentials of halomethanes measured by fluorescence quenching experiments. Royal Society of Chemistry, **2000**. *7*: p. 1583-1595.

49. Fukuzumi, S. and J. Maruta, Electron transfer reduction of cobalt tetraphenylporphyrin by hydroquinone dianions and alkylation with alkyl halides. Inorganica Chimica Acta, **1994**. *226(1-2):* p. 145-150.

50. Roberts, A.L., Burris, D.R., Delcomyn, C.A. and Smith, M.H., Reductive Dechlorination of Tetrachloroethylene and Trichloroethylene Catalyzed by Vitamin B_{12} in Homogeneous and Heterogeneous Systems. Environmental Science and Technology, **1996**. *30:* p. 3047-3052.

51. Totten, L.A. and A.L. Roberts, Calculated one- and two-electron reduction potentials and related molecular descriptors for reduction of alkyl and vinyl halides in water. Crit. Rev. Environmental Science and Technology, **2001**. *31*: p. 175-221.

CHAPTER II

TUNING THE REACTIVITY OF FLAVIN MONONUCLEOTIDE (FMN) TOWARDS TRICHLOROETHYLENE

2.1 Introduction

2.1.1 Molecular Catalysts for Environmental Remediation

Reductive dehalogenation reactions are presently of great interest because of their potential use in the treatment of halogenated solvent wastes. The degradation of organohalide pollutants via catalytic reductive dehalogenation processes can be carried out with the aid of molecular catalysts. Organohalides can react with a variety of molecular catalysts, for example, transition metal macrocycles containing Fe(II), Fe(I), Co(I) and Ni(I) [1-3]. Recently, it also has been reported that certain bacterial species can use PCE and TCE as electron acceptors by reducing it to *cis*-dichloroethylene catalyzed by an enzyme PCE reductase that contains a corrinoid [4-7]. Some studies have suggested that corrinoids are potent reductants for chlorinated compounds [3, 8]. The super-reduced corrinoids acts as strong nucleophiles that can react by nucleophilic substitution, addition, or electron transfer mechanisms with halogenated compounds. The advantage of using corrinoids as electron mediators in waste water treatment is the rapid regeneration of the reactive corrinoid species without significant loss of activity over long time periods and no accumulation of toxic products.

Schwarzenbach et al. has shown that homogeneous aqueous solutions containing the molecular catalysts cobalamin, cobinamide, and cobamide in the presence of titanium(III) citrate or titanium(III)-NTA as bulk electron donor, are effective electron transfer mediators for the reduction of PCE, TCE and TCFE [3]. Wilfred van der Donk reported possible mechanisms for the dechlorination of PCE through electron transfer and nucleophilic attack pathways. Based on van der Donk's work, it was observed that the catalytic dechlorination of PCE is a one-electron transfer from cob(I)alamin to PCE [9]. The ability of molecular catalysts to mediate electron transfer towards degradation of organohalides is a promising area of research. Therefore, it is desirable to design a molecular catalyst that is capable of degrading organohalides in the presence of reducing agents. In this chapter, the reduction of organohalides (RX) by the molecular catalyst Flavin mononucleotide (FMN) is described.

2.1.2 Flavin Mononucleotide

Since their discovery in the 1930s, flavins have been recognized as being capable of electron transfer processes, and thus they play a crucial role in the coupling the two-electron oxidation of most organic substrates to the one-electron transfers of the respiratory chain [10-13]. Flavins are redox active chromophores found in many enzymes and photoreceptors, e.g. the flavin enzymes or flavoproteins which occur widely in animals and plants [10, 13-15]. Many of these flavoproteins work directly on the substrates, while others act as intermediates in the respiratory chain by bridging the

electron-transport gap between the pyridine nucleotides which they dehydrogenate, and the cytochromes, to which they transfer the hydrogen [14].

Riboflavin, which occurs exclusively in nature is also commonly known as vitamin B_2 (6,7-dimethyl-9-ribitylisoalloxazine). Riboflavin is water-soluble and participates in redox reactions typically, as a hydrogen carrier in the process of carbohydrate, protein, and fat metabolism, synthesis of hemoglobin and maintenance of the visual function of the eye [10, 13, 14]. The name riboflavin is derived from the ribityl side chain and the yellow color of the conjugated ring system. Deprivation of riboflavin in humans causes disturbance of growth, skin diseases and hair loss [10]. The flavin group constitutes a part of hydrogen transferring coenzymes, i.e. flavoenzymes, which are linked with the apoproteins.

Two of the common flavoenzymes derived from riboflavin are flavin mononucleotide (FMN) and flavin-adenine dinucleotide (FAD), which are commonly called flavin nucleotides. Existing both free in solution and bound to protein, they function in a wide range of oxidation-reduction reactions [16]. One class of flavoproteins, flavodoxins (Fld), are small (15-20 kDa) electron transferring proteins that have the flavin mononucleotide (FMN) as the redox cofactor noncovalently bound to a single polypeptide [17]. The structure of flavin mononucleotide is shown in Figure 2.1.

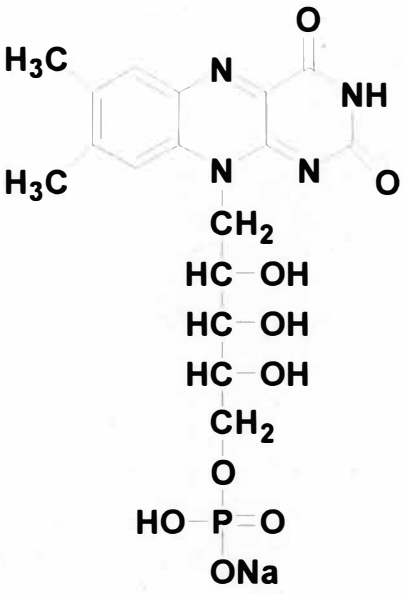

Figure 2.1 Structure of Flavin Mononucleotide (FMN)

Flavin mononucleotide (riboflavin 5'-monophosphate) is a coenzyme of the respiratory complex I (NADH-coenzyme-Q-reductase) of mitochondria membranes [18] and of many other electron transfer enzymes [19]. FMN is a cofactor in the phototrophins of plants, which are the blue-light sensitive photoreceptors responsible for phototropism, chloroplast movement, stomata opening, rapid inhibition of stem growth, and gametogenesis [18].

Flavins possess three readily accessible oxidation states: the fully oxidized flavoquinone (Fl_{ox}); the flavosemiquinone radical, in either the anionic red (Fl_{red}^{-}) or neutral blue ($Fl_{rad}H$) form with a pKa of 8.5 [10]; and the two electron reduced flavohydroquinone, which can exist in anionic red ($Fl_{red}H^{-}$) or neutral blue ($Fl_{red}H_2$) form [16, 20-22]. This versatility depends in part on their ability to form the semiquinone structure and thus function as centers for both one-electron and two-electron transfer

reactions. Figure 2.2 shows the different redox structures, each with the associated protonation state that occurs in the physiological pH range.

Flavins are extremely sensitive to light. Upon absorption of light, hydrogen is transferred from the hydroxylic side chain to the isoalloxazine ring with the side chain being subsequently split off [14]. The isoalloxazine moiety forms a reversible redox system as show by polarographic technique [24]. Potentiometric titration curves for FMN in the pH range of 0.89 and 10.9 as conducted by Lowe and Clark suggested that the oxidation-reduction process is reversible and involves the formation of a semiquinone as an intermediate in the 2 (two) equivalent change [25].

The reduced flavin can be re-oxidized, either in two-electron steps or a single electron step. In some enzymes, molecular oxygen is the physiological substrate, i.e. it can be reduced by the reduced flavin. For this reason, the reductive half reactions as well as other reactions of reduced flavins with specific substrates, are studied under anaerobic conditions. The crystal structure of oxidized and reduced flavins was solved at 2.0 Å resolution and showed the geometry of the oxidized FMN cofactor to be planar, while 1.5-dihydroFMN is bent along the N_5, N_{10} axis [26] (Figure 2.2).

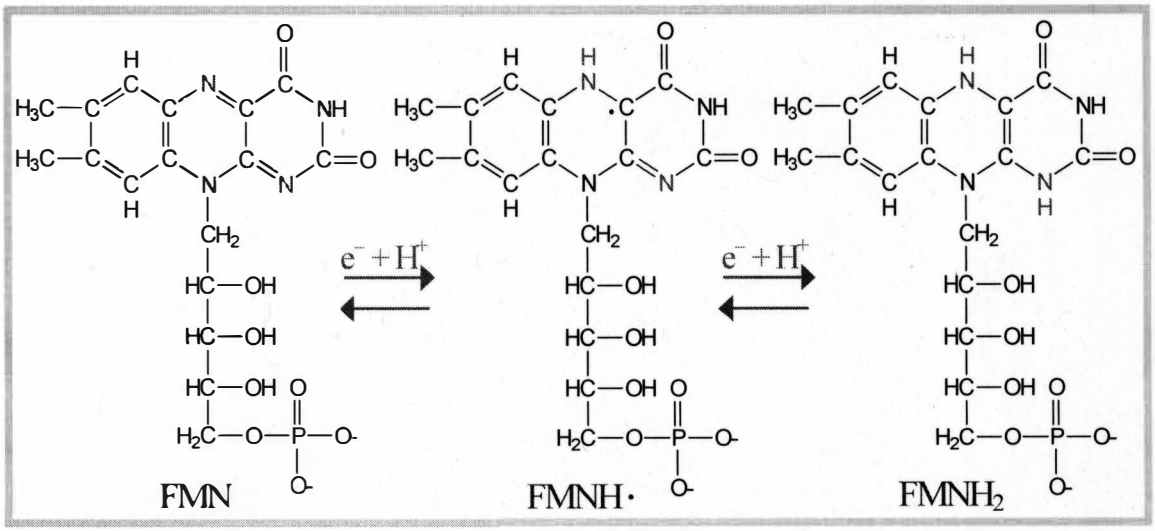

Figure 2.2 Various redox states of FMN: oxidized FMN, FMNH· semiquinone and reduced $FMNH_2$

The ability of FMN to engage in one- as well as two-electron transfer reactions enables flavins to act as transformers between obligate $2e^-$ donors (e.g., NADH) and obligate $1e^-$ acceptors (e.g. heme Fe) [27]. By controlling the switches between one- and two-electron processes, one can study the reactivity of FMN in catalyzing the reduction of organohalides (RX).

2.1.3 Mechanism of Electron Transfer for Reduction of Organic Compounds

The chemistry behind electron transfer mechanisms in organohalide pollutants is of considerable interest to environmental chemists [28-31]. Even though the reduction of organic contaminants has been studied extensively, detailed molecular level descriptions

of electron transfer mechanisms are still lacking. By fully understanding the electron transfer mechanisms, it allows one to predict and control organohalide redox reactions.

Under anaerobic conditions, two electron transfer mechanisms for the reduction of organohalides have been reported to be stepwise and dissociative mechanisms [8, 32]

1. Stepwise mechanism

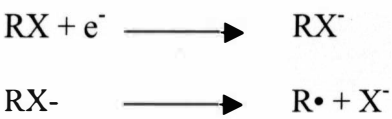

2. Dissociative mechanism

During the stepwise electron transfer mechanism, a reduced organohalide (RX^-) intermediate is produced [8]. In the case of a dissociative electron transfer mechanism, electron transfer and C-X bond cleavage occur in a concerted process. The dissociative mechanism is generally thought to be irreversible and was predicted to be more favorable than the stepwise mechanisms for some organohalides, such as perchloroethylene (PCE) and trichloroethylene (TCE) [8, 32]. Part of the explanation is that the standard potentials and reorganization energies for the concerted and stepwise pathways in the electrochemical reduction of PCE and TCE are not the same.

Saveant et al. found that the stepwise pathway of electron transfer has more negative reduction potentials compared to the dissociative pathway for perchloroethylene (PCE), $E^0(C_2Cl_4/C_2Cl_4^-)$ = - 1.71 V and E^0 $(C_2Cl_4/C_2Cl_3\bullet + Cl^-)$ = - 1.33 V vs. NHE,

respectively. It was concluded that the electrochemical reaction follows the stepwise pathway rather than the concerted/dissociative pathway because the value found for the measurement of attractive interaction between the caged fragments upon fitting the experimental data is too large compared to other compounds such as polychloroalkanes. The results indicated that the dissociative electron transfer was energetically more favorable than the stepwise process.

2.2 Experimental Section

2.2.1 Materials and Reagents

Riboflavin 5'-monophosphate sodium salt dihydrate (FMN), methanol (CH_3OH)≥99%, trichloroethylene (anhydrous)≥99%, and tetrabutylammonium hexafluorophosphate ($TBAPF_6$) were obtained from Sigma Aldrich. Anhydrous methanol was prepared by soaking molecular sieves in the methanol solution {±60} minutes and used as prepared. Deionized Milli-Q water at a pH of ~7 was used where aqueous measurements are described. Absorption and emission spectroscopic studies were carried out at neutral pH.

Standard quartz cuvettes with a 1-cm path length with all sides polished were used for UV-visible absorbance and fluorescence measurements. A solution of aqua regia (3:1 v/v HCl: HNO_3) was used to clean the quartz cuvette prior to use. Hamilton syringes (500 μL and 250 μL) were purchased from VWR International.

2.2.2 Instrumentation

UV-visible absorption spectra were acquired using a Varian Cary 50 spectrophotometer. Fluorescence measurements were acquired using Varian Cary Eclipse Fluorescence spectrometer using an excitation wavelength of 350 nm (spectral width of interference filter 5 nm).

Irradiation of FMN solutions in either methanol or water, were carried out using a solar simulator equipped with 400W Xenon lamp and 21.7 kA with a KV-370 filter purchased from Newport, Inc. (Spectra-Physics, Stratford CT). A 4 mL of a solution of FMN was placed in a standard 10 mm x 10 mm quartz cuvette, sealed with a rubber septum, and purged with ultra high pure compressed N_2 (Airgas, inc). In each case, samples were irradiated for 30 min under a N_2 atmosphere. Irradiation was continued until the sample showed no fluorescence under UV light, thus indicating complete reduction.

2.2.3 Spectroelectrochemistry/Electrochemistry

Sweep mode cyclic voltammetry was conducted on a CV 50W Potentiostat (BAS Bioanalytical System, Inc), in a three-cell arrangement consisting of a Pt gauze counter electrode, a glassy carbon working electrode and Ag/AgCl reference electrode. For supporting electrolytes, 0.1 M tetrabutylammonium hexafluorophosphate ($TBAPF_6$) was used in non-aqueous solution, while 0.1 M NaCl was used in aqueous solution. For each measurement, the sample was placed in an electrochemical cell compartment pre-washed with aqua regia. Each sample was purged for 10 minutes with nitrogen. A solution

consisting of supporting electrolytes dissolved in either methanol or aqueous solution was used as a blank, and was run prior to each measurement.

For spectroelectrochemical measurements, 5 x 10^{-4} M of FMN solution in methanol was placed in a thin layer quartz crystal spectroelectrochemical cell (CH Instruments, Inc). Spectroelectrochemical measurements were conducted on a CV 50W Potentiostat to apply the desired potentials in a standard three-electrode arrangement with a Pt counter electrode, Ag/AgCl reference electrode (3M KCl), and Pt gauze electrode. All measurements were carried out under a N_2 atmosphere. A Cary 50 Spectrophotometer was used to measure absorbance spectra of the solution following an applied potential. Each potential was held until the UV-visible absorbance spectrum remained unchanged.

2.2.4 Steady-State Kinetic Analysis of Trichloroethylene Reactivity

A Varian Cary 50 UV-visible absorbance spectrophotometer was used to acquire steady-state spectra for the reaction of $FMNH_2$ with TCE. An aliquot of N_2 saturated TCE in methanol solution (0.115 M, 0.223 M, and 0.668 M) or TCE in aqueous solution (0.115 M, 0.223 M, and 0.668 M) was added to FMN in either a methanol or an aqueous solution. The appearance of a 515 nm and 520 nm absorbance of FMN and the disappearance of the 450 nm absorbance peak corresponding to $FMNH_2$ were monitored. Pseudo-first order kinetic rate constant, k_{obs} were obtained by fitting to equation 2.1. Analysis was conducted using a scientific graphic and analysis software ORIGIN version 7.5.

$$\ln A = \ln A_0 - k_{obs}\, t \qquad \text{(Eq. 2.1)}$$

Where A = absorbance, A_0 = initial absorbance, t = time, and k_{obs} = observed rate constant

2.3 Results and Discussion

2.3.1 UV-Visible Absorbance and Fluorescence Spectra of Flavin Mononucleotide

The absorption spectrum of flavin mononucleotide in methanol solvent and aqueous solution shows absorption maxima at 355 and 445 nm as shown in the Figure 2.3, in good agreement with the spectrum of free FMN [10]. These peak maxima are due to $\pi - \pi^*$ electronic transition of the double bond in the isoalloxazine group [33]. The presence of the two (2) $\pi - \pi^*$ transitions in the 450 nm and 360 nm region is predicted by MO theory and supported by circular dichroism and polarized fluorescence excitation spectra [33]. The molar absorptivities of FMN was calculated to be 7,483.6 $\pm$ 85.3 M^{-1} cm^{-1} at 355 nm and 10,385.5 $\pm$ 217.1 M^{-1} cm^{-1}at 445 nm in agreement with the literature [34, 35].

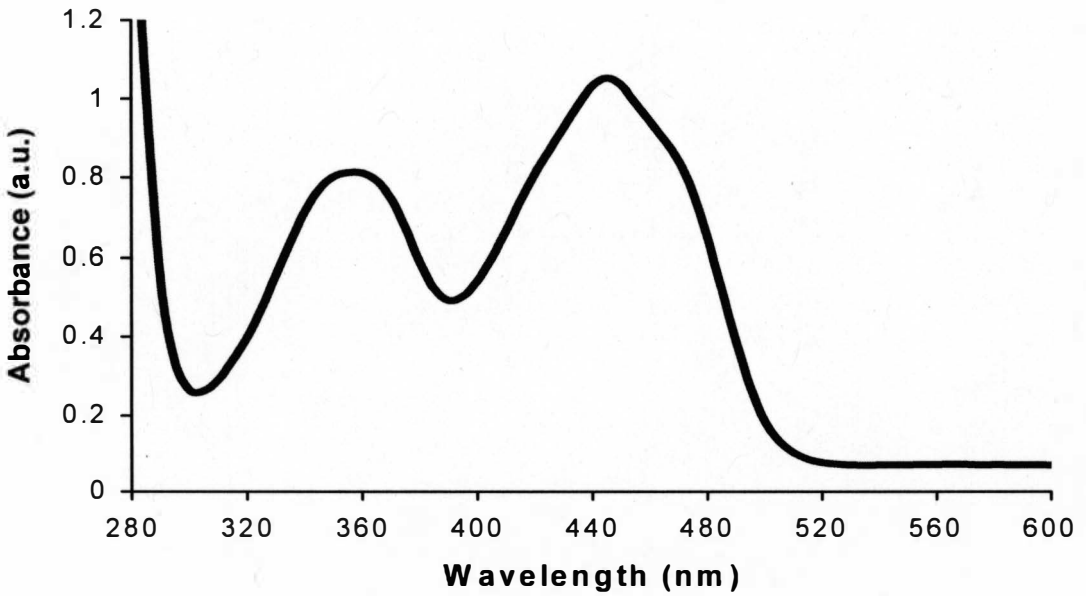

Figure 2.3 UV-visible absorbance spectrum of 0.0001 M of FMN in methanol at room temperature

A distinctive characteristic of oxidized free flavins is their relatively strong fluorescence (quantum yield ~0.3) accompanied by an emission maximum typically around 520 nm [33]. The energy and intensity of this emission are dependent on solvent polarity and temperature, on formation of complexes with a variety of molecules, and on the position and properties of substituents [21, 33]

The fluorescence spectrum of flavin mononucleotide shows an emission maximum at 525 nm (under 350 nm excitation wavelength).as displayed in Figure 2.4. Similar observations were reported by Massey et al who recorded the fluorescence emission in the range of 476-512 nm at 77 K for reduced model flavins [21]. The fluorescence states of isoalloxazines have been characterized as $^1(\pi - \pi^*)$ and $^3(\pi - \pi^*)$

types, on the basis of polarized fluorescence and phosphorescence spectra in ethanol at 77K.

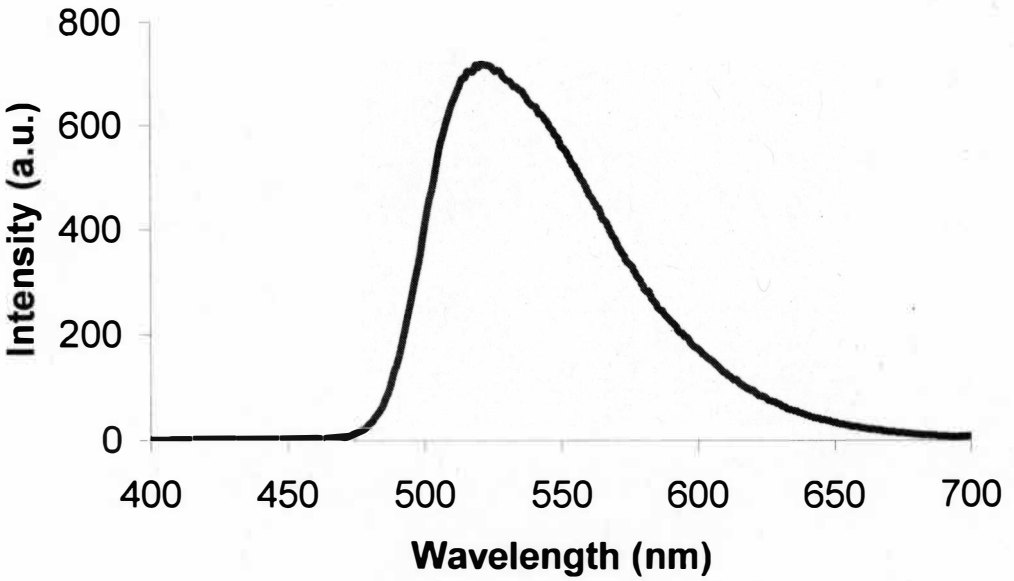

Figure 2.4 Fluorescence spectrum of 0.0001 M of FMN in methanol at room temperature

2.3.2 Photoreduction of FMN in Methanol Solvent

The photoreduction of flavin mononucleotide (FMN) to $FMNH_2$ is a well-known two-electron two-proton process [10, 36], which is accompanied by changes in absorption and emission wavelengths and intensities. The fluorescence and visible color changes of FMN before and after irradiation (to form $FMNH_2$) are shown in Figure 2.5. The transition of color from the original intense yellow color to colorless indicates the formation of reduced flavin as reported by earlier works [37-39].

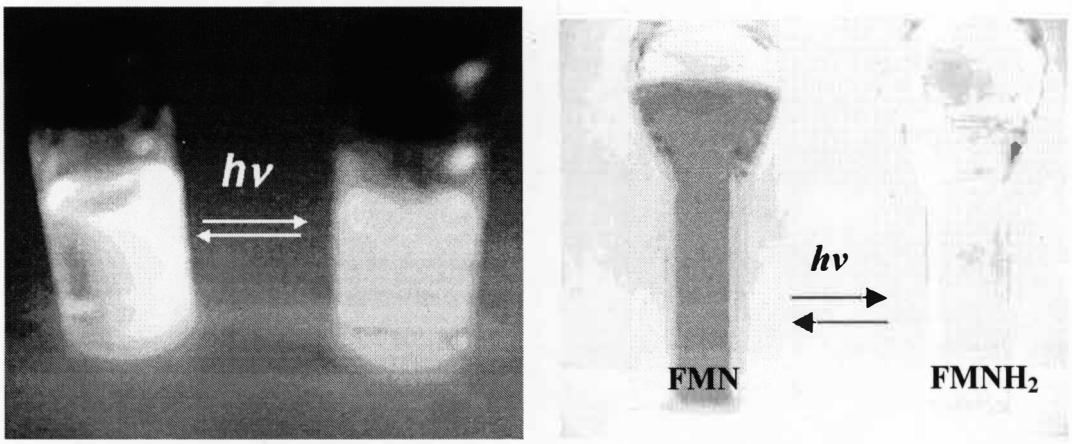

Figure 2.5 FMN is photochemically reduced to $FMNH_2$ in methanol solvent. Left: Photograph of the fluorescence color change of FMN and $FMNH_2$ (after irradiation) taken under UV light. Right: Photograph of the visible color changes of FMN and $FMNH_2$ (after irradiation)

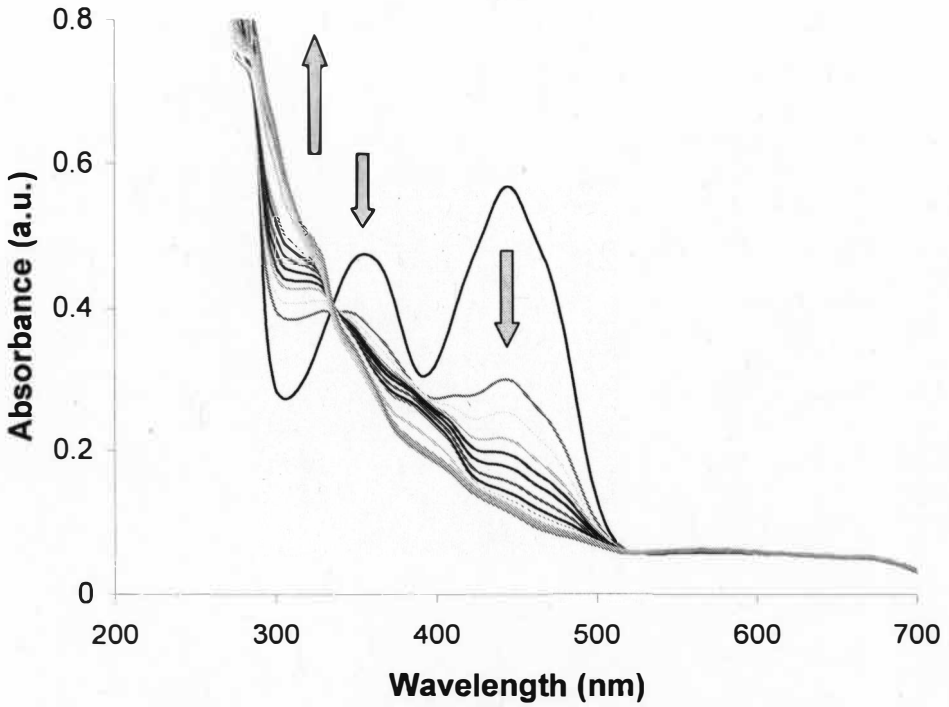

Figure 2.6 Changes in the UV-visible absorbance spectra of FMN as it is reduced photochemically in methanol solvent to $FMNH_2$. (Measurements were taken in 90 second increments)

UV-visible absorbance spectra of photoreduction of FMN to $FMNH_2$ in methanol solvent are shown in Figure 2.6. The sample was irradiated and measurements were recorded in 90 second time intervals. It was observed that FMN was gradually reduced to the semiquinone FMNH• and eventually into fully reduced hydroxyquinone, $FMNH_2$. The intensity of FMN absorbance decreases with increase in irradiation time resulting in the formation of a new peak.

The UV-visible absorbance spectrum of $FMNH_2$ shows a peak in the 280-300 nm regions, while the emission spectrum represents a peak at 450 nm. Upon exposure to air, this reduced form $FMNH_2$ reacts quickly with molecular oxygen to become FMN [40]. Isosbestic points at 280 and 330 nm were observed where FMN and $FMNH_2$ have the same absorptivity at the specific wavelength. At this isosbestic point, there is an equal concentration of both species FMN and $FMNH_2$.

A similar pattern in the absorption spectra of successive oxidation states from fully reduced to fully oxidized FMN in 0.25 M citrate at pH 6.1 was reported in the literature [12].

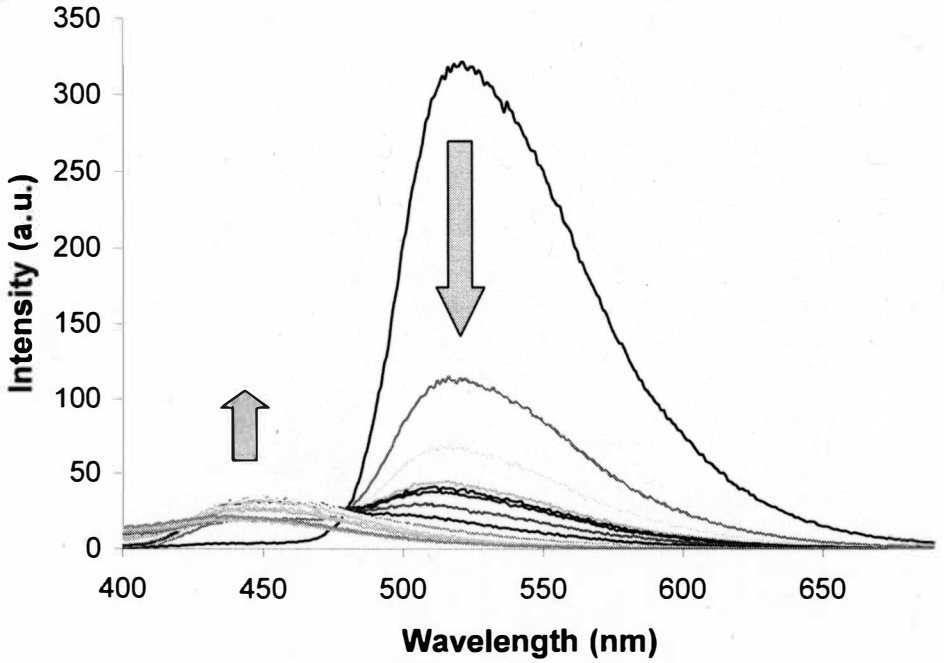

Figure 2.7 Fluorescence spectra of FMN irradiation to $FMNH_2$ in methanol in 30 minutes with increments of 90 seconds

Emission spectra of FMN reduced photochemically to $FMNH_2$ in methanol solvent are shown in Figure 2.7. The emission spectrum of FMN shows a peak maximum at 525 nm. Following continuous irradiation, FMN is converted into $FMNH_2$ accompanied by the blue shift (hypsochromic shift) of the emission spectrum and the emergence of a new peak at 448 nm. Both FMN and $FMNH_2$ display distinct fluorescence colors as shown in the figure below (FMN fluoresces green, while $FMNH_2$ fluoresces blue).

2.3.3 Spectroelectrochemistry of FMN in Methanol Solvent

Spectroelectrochemistry is an analytical technique that combines electrochemistry with spectroscopy. Since the first reported spectroelectrochemical study, apparatus and methodology have been developed for application to virtually every region of the electromagnetic spectrum. To date, a vast majority of studies have been performed in the ultraviolet/visible (UV-visible) and infrared (IR) regions. Spectroelectrochemical (SEC) cells for UV-visible and IR applications typically employ either transmittance or external reflectance sampling, the former being more common for examination of solution species and the latter for electrode surface studies [41]. Surprisingly, to date there are very few reports on the spectroelectrochemical redox studies of flavin [17,23].

In this work, a spectroelectrochemical study was conducted to provide an appropriate method to analyze the reduction of FMN to $FMNH_2$ at the surface of a working electrode, in this case Pt wire gauze. The SEC-cell thin layer used in this study is shown in Figure 2.8. As mentioned earlier, the reference electrode used in this study is a Ag/AgCl (3 M KCl) electrode. All measurements were made at 25 °C.

Figure 2.8 b shows the UV-visible spectroelectrochemical data of a 5.0×10^{-4} M FMN in methanol solution in 0.1 M $TBAPF_6/CH_3OH$ supporting electrolyte.

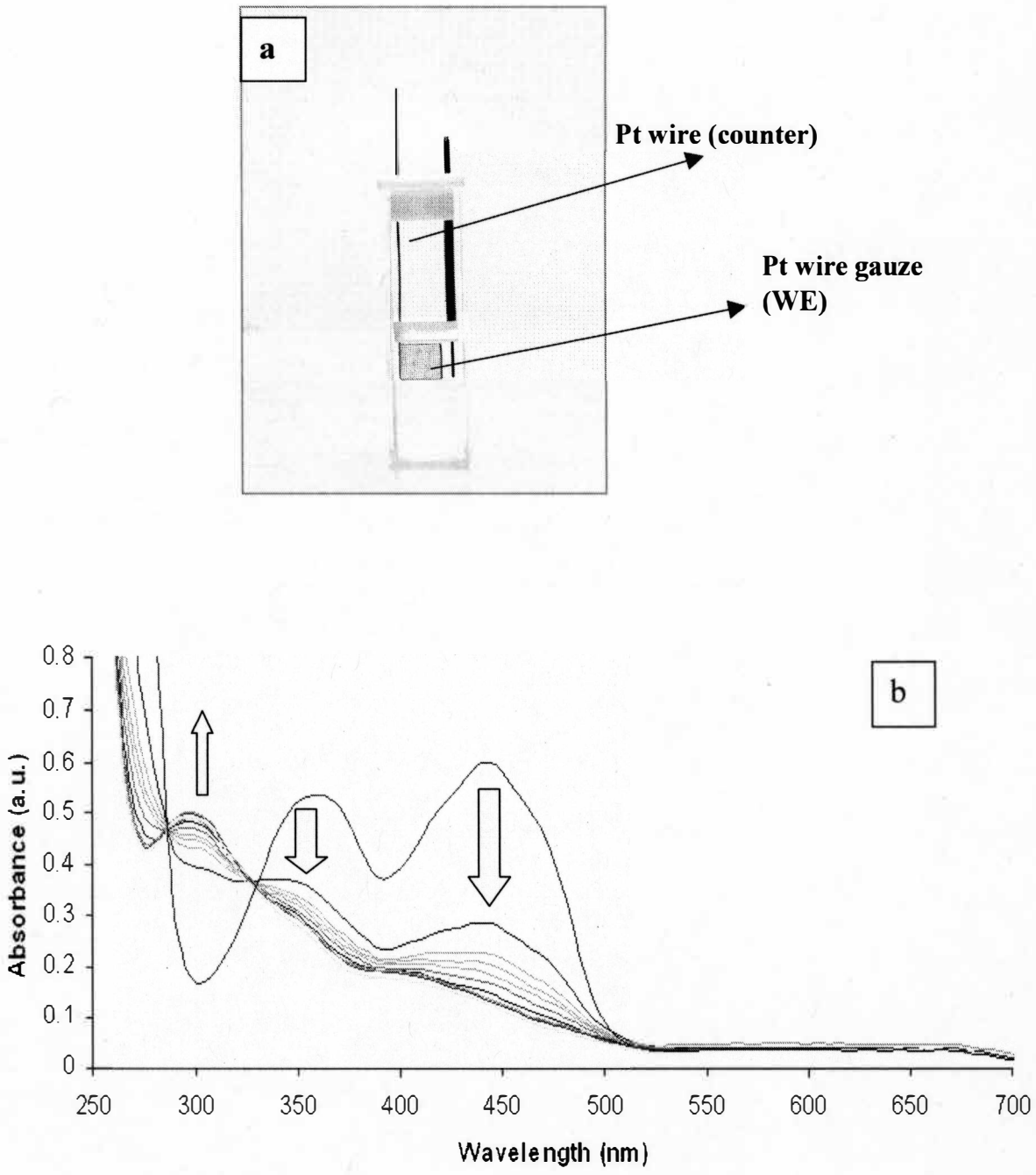

Figure 2.8 (a) SEC-Cell Thin Layer purchased from CH Instruments (b) UV-visible absorbance spectroelectrochemistry of FMN in $TBAPF_6/CH_3OH$ at a concentration of 5.0×10^{-4} M. The reductive potential applied = -1000 mV vs. Ag/AgCl (3M KCl)

The data suggest that FMN can be cycled through its oxidized, semiquinone, and hydroxyquinone states by the application of an electrical bias. The negative applied potential was –1000 mV, with the film being allowed to stabilize for 5-10 minutes before the optical spectrum was recorded. Complete stabilization of the absorbance spectrum was observed within a 20-minute period for all biases, indicating that all electroactive species reached thermodynamic equilibrium with the electrode within this time scale.

The application of potentials up to –1000 mV vs. Ag/AgCl results in the appearance of a broad absorption band between 300 and 500 nm, characteristic of the formation of the neutral semiquinone FMNH•, which fluoresces blue in color [35]. Upon the application of more negative potentials, these broad absorption bands disappeared, and formation of a new band at 280 – 300 nm characteristic of the formation of the flavin hydroxyquinone, $FMNH_2$, was observed.

This result confirmed that FMN can be partially reduced to its semiquinone radical FMNH•, and then completely reduced into a fully reduced $FMNH_2$ on the surface of the Pt wire gauze working electrode by applying a potential of –1000 mV. Similar results were obtained earlier from a photochemical reduction experiment where FMN was reduced to FMNH• followed by $FMNH_2$.

2.3.4 Reactivity of $FMNH_2$ in Methanol Solvent

In methanol solvent, FMN can undergo two-electron reduction accompanied by two-proton reduction to $FMNH_2$ and thus carries two electrons [21, 42]. This system of $FMNH_2$ in methanol solvent is very reactive and thus will reduce TCE by delivering the accumulated electrons.

Schematically, the reaction proceeds as the following:

$$FMN \rightleftharpoons FMNH_2$$

$$FMNH_2\,(2e^-) + TCE \rightleftharpoons FMN + (TCE)^{2-}$$

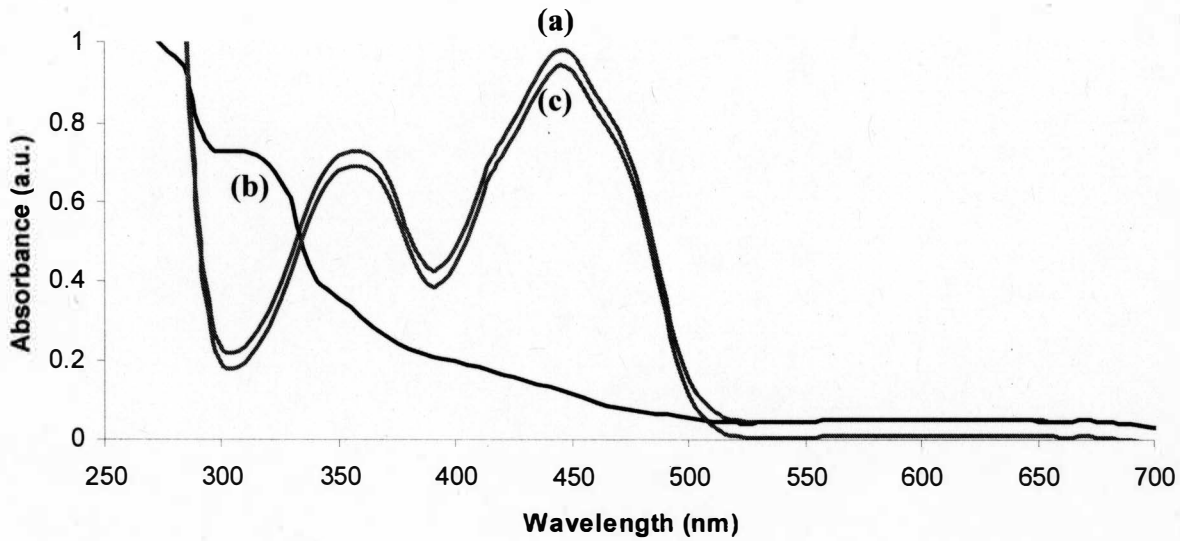

Figure 2.9 UV-visible absorbance spectra of 0.001 M $FMNH_2$ in methanol, (a) before irradiation (b) after irradiation, and (c) after the addition of TCE in the *dark*

The UV-visible absorbance spectra on Figure 2.9 show the reactivity of the reduced flavin $FMNH_2$ with TCE. 10^{-5} M TCE was added to a deareated solution of $FMNH_2$ causing the reemergence of the peaks at 355 and 445 nm. The reemergence of both peak shows that $FMNH_2$ was oxidized back to FMN, followed by the reduction of TCE. This result is important because it shows that FMN reacts as a catalyst in electron transfer process as the electrons in the reduced flavin are being transferred back to FMN ($FMNH_2$ undergoes oxidation, loss of electrons) and as a result TCE is reduced.

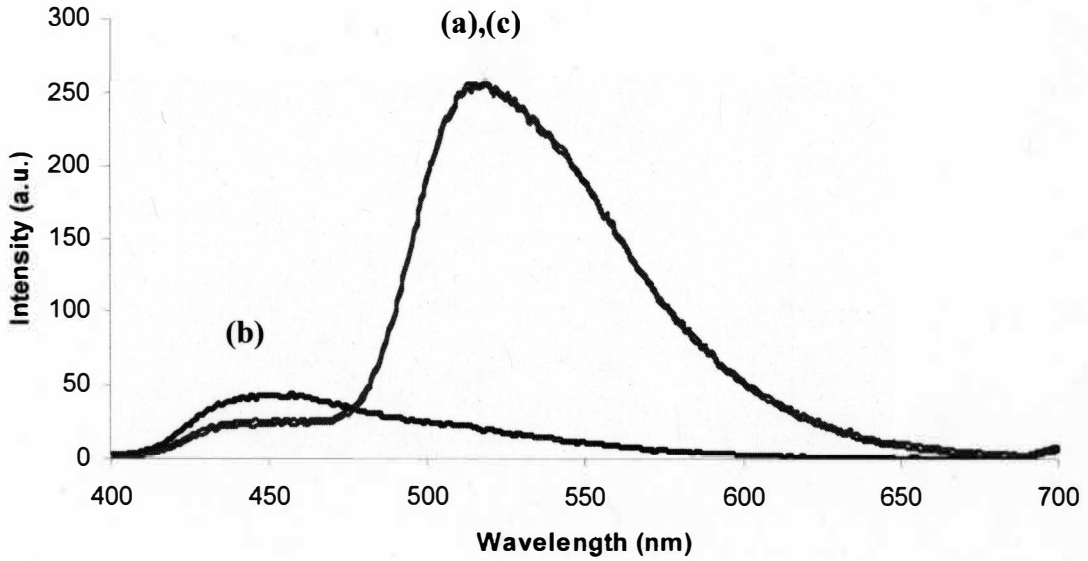

Figure 2.10 Fluorescence spectra of 0.001 M of FMN in methanol (a) before irradiation, (b) after irradiation and (c) after addition of TCE in the *dark*

This result was further supported by fluorescence spectra of FMN as shown in Figure 2.10. From the spectral data, it was observed that the 520 nm peak reemerges following TCE injection to the reduced flavin $FMNH_2$. This result means that the re-

oxidation of $FMNH_2$ to FMN occurs and accompanied by the reduction of TCE. The rate of TCE reduction was calculated by conducting steady-state fluorescence kinetics. The fluorescence kinetic result is shown in Figure 2.11 below.

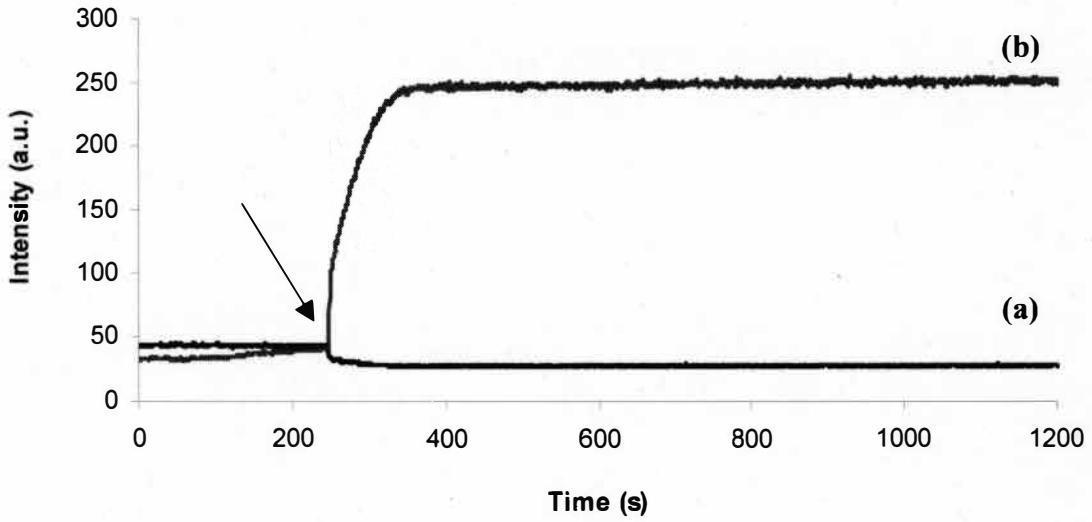

Figure 2.11 Steady-state kinetic fluorescence spectra monitored at (a) 445 nm ($FMNH_2$), and (b) 525 nm in methanol solvent. The arrow line indicates the time where TCE was injected

Following TCE injection, the 445 nm peak corresponding to $FMNH_2$ decreased in intensity, whereas the 525 nm oxidation peak increased in intensity. This observation supported the notion that $FMNH_2$ was re-oxidized to FMN and was further accompanied by TCE reduction. It has been shown clearly that in the presence of $FMNH_2$ carrying 2 electrons, TCE reactivity was observed. This is due to the strong reducing nature of $FMNH_2$.

Pseudo-first order kinetic rates, k_{obs} were obtained by fitting the steady state UV-visible absorbance and fluorescence data to equation 2.1. The reduction rate constant (k) of TCE degradation was analyzed by plotting k_{obs} vs. concentration of TCE since the reactions were pseudo-first order in FMN. The slope of the graph generated from this plot is the corresponding reduction rate constant. In this particular system, the reduction rate constant of TCE is calculated to be 0.5 M^{-1} s^{-1} as seen on Figure 2.12.

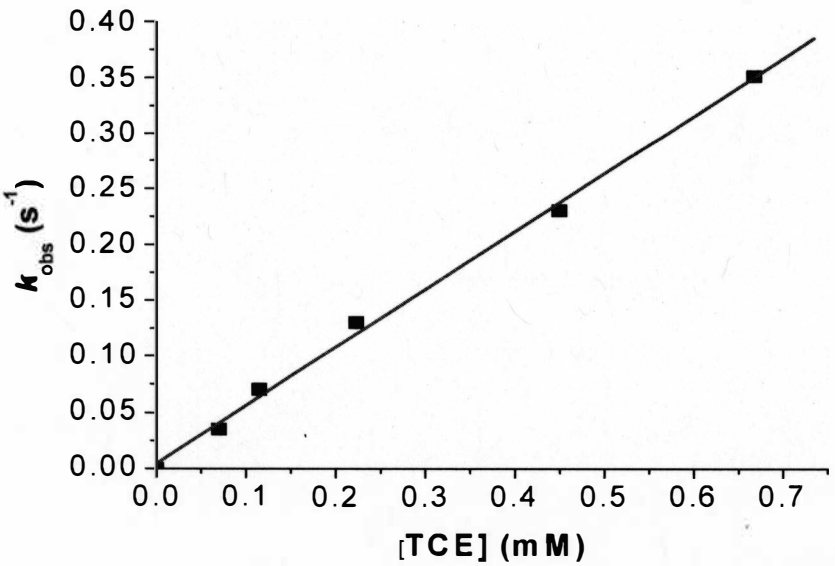

Figure 2.12 Plot of reduction rate constant (k) of TCE on $FMNH_2$ catalyst in methanol solvent as a function of k_{obs} vs. concentration of TCE

2.3.5 Reactivity of FMNH· in Aqueous Solution

The behavior of FMN in aqueous solution is different than in methanol solution. In aqueous solution, irradiation of FMN resulted in the formation of a semiquinone radical FMNH·. Michaelis stated that riboflavin (constituent of FMN) could give rise to semiquinone free radicals by the action of one-electron reducing agents [38]. The mechanism by which the transfer of electrons takes place was investigated earlier by which one electron transfer was connected with a proton transfer [42, 43]. This semiquinone radical formed here at pH~7 is a neutral semiquinone [16, 44] and it is stable in the range of pH 2.3 to 8.3 [45]. Michaelis and Kuhn suggested that the semiquinone radical intermediates have a considerable lifetime under certain conditions.

The kinetics of reactions have been extensively studied in aqueous solvent using various techniques such as temperature jump [46] and pulse radiolysis [47]. Swallow and Land studied the formation of FMNH· and $FMN^{\cdot -}$ in aqueous solution by pulse radiolysis experiments [47]. The investigation have underlined the importance of the formation of a dimer $F\text{-}FH_2$ which is the precursor to the formation of FMNH· semiquinone radical. All primary products of water radiolysis lead ultimately to the reduction of flavin to semiquinone FMNH·. Based from these analysis, it was conclusive that in aqueous solution, FMN can be partially reduced into a semiquinone radical FMNH· form through the conversion of the primary radicals formed on water radiolysis into flavin semiquinone radicals. The reduction scheme of FMN to FMNH· semiquinone radical in aqueous solution and the corresponding photographs are shown in Figure 2.13 and Figure 2.14.

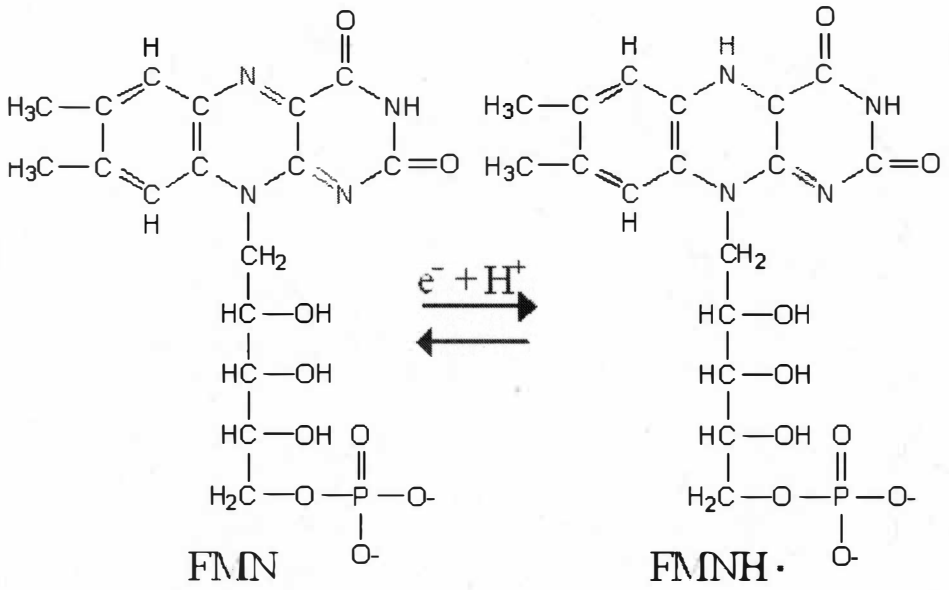

Figure 2.13 Photoreduction of FMN to FMNH· semiquinone radical in aqueous solution

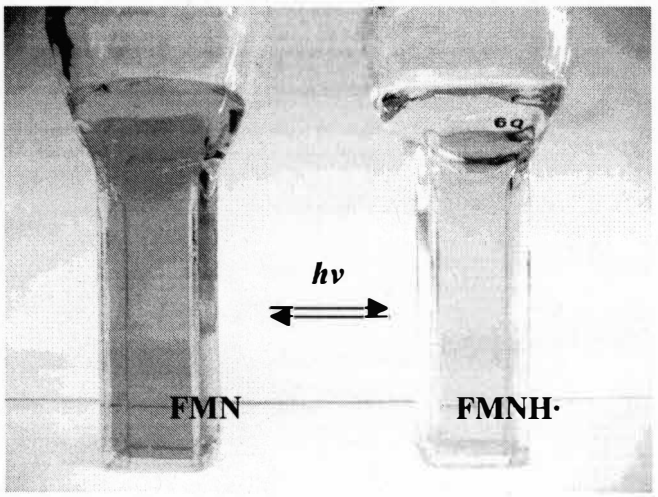

Figure 2.14 Photograph of FMN and FMNH· semiquinone radical in aqueous solution.

The study of TCE degradation using FMN was conducted using UV-visible absorbance and fluorescence spectroscopy as shown in Figure 2.15 and Figure 2.16.

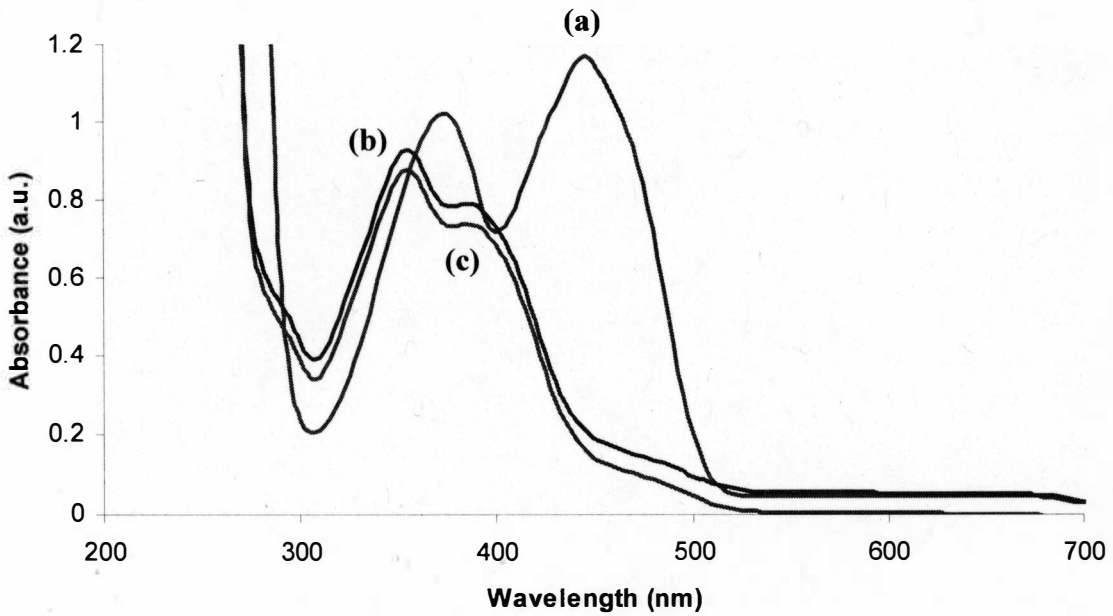

Figure 2.15 UV-visible absorbance spectra of FMN in aqueous solution (a) before irradiation, (b) after irradiation, and (c) after addition of TCE in the *dark*

The half-reduced semiquinone radical FMNH· shows no reactivity towards TCE and does not participate in the electron transfer process. UV-Visible absorbance spectrum indicates that the addition of 10^{-5} M TCE into the semiquinone radical FMNH· shows no reactivity towards TCE. The result showed that the presence of one electron is not strong enough of a reducing agent to reduce TCE.

Schematically, the reaction proceeds as the following:

$$FMN \rightleftharpoons FMNH\cdot$$

$$FMNH\cdot + TCE \rightleftharpoons \text{No reactivity}$$

This result was further supported by fluorescence spectrum of FMN where the λ = 520 nm peak does not reappear as the TCE is injected to the partially reduced flavin FMNH· as shown in the Figure 2.16.

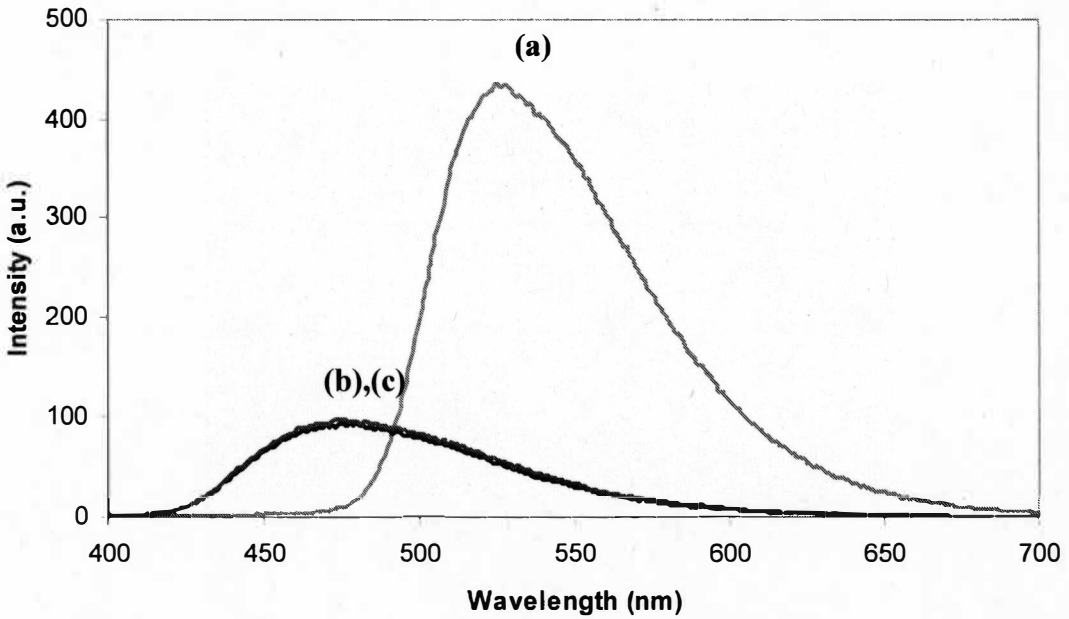

Figure 2.16 Fluorescence spectra of FMNH· produced by FMN irradiation in aqueous solution (a) before irradiation, (b) after irradiation, and (c) after addition of TCE in the *dark*

The rate of FMNH· oxidation to FMN was analyzed using steady-state kinetics to monitor TCE reactivity in the system. The excitation wavelength is 350 nm and multiple

wavelengths were monitored: 460 nm ($FMNH_2$) and 525 nm (oxidized FMN). Kinetics was monitored for 1200 seconds. The fluorescence kinetic result is shown in the Figure 2.17.

Following TCE injection, no changes on the steady state kinetic was observed. In aqueous solution, FMNH· does not get oxidized back to FMN and TCE does not get reduced. The radical semiquinone FMNH· is not strong enough of a reducing agent to reduced TCE. Therefore, there is no change observed on the steady state kinetics following the injection of TCE.

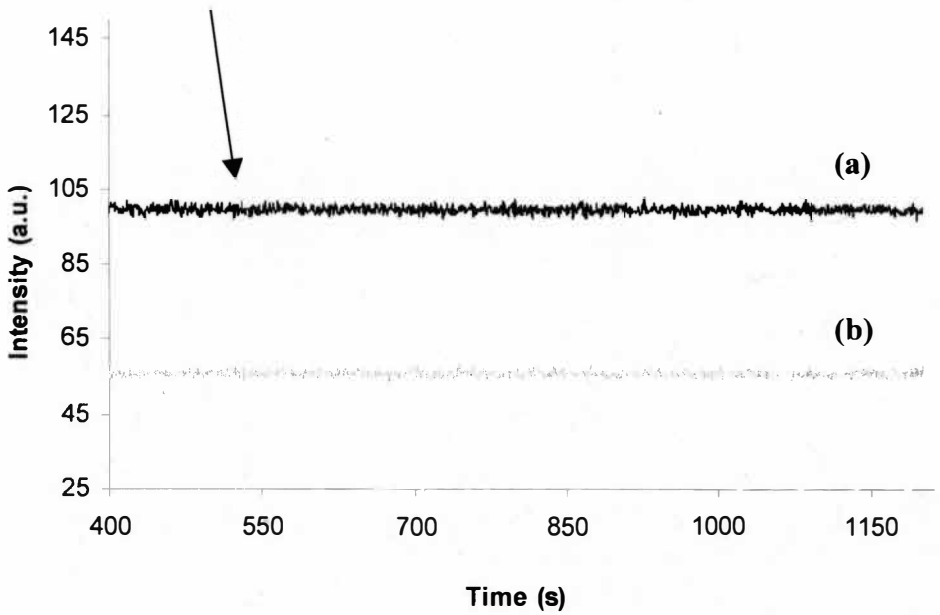

Figure 2.17 Steady-state kinetic fluorescence spectra monitored at (a) 445 nm and (b) 525nm. The arrow lines indicate the time where TCE was injected

2.3.6 Electrochemistry of FMN in Methanol and in Aqueous Solutions

Cyclic voltammograms of FMN in methanol and FMN in aqueous solution are shown in Figure 2.18. When the potential becomes more negative, -0.2 V, a cathodic current develops due to the reduction of FMN to $FMNH_2$. The anodic current results from the re-oxidation of $FMNH_2$ to FMN that has accumulated near the surface during the forward scan. This anodic current peaks and then decreases as the accumulated $FMNH_2$ are used up by the anodic reaction.

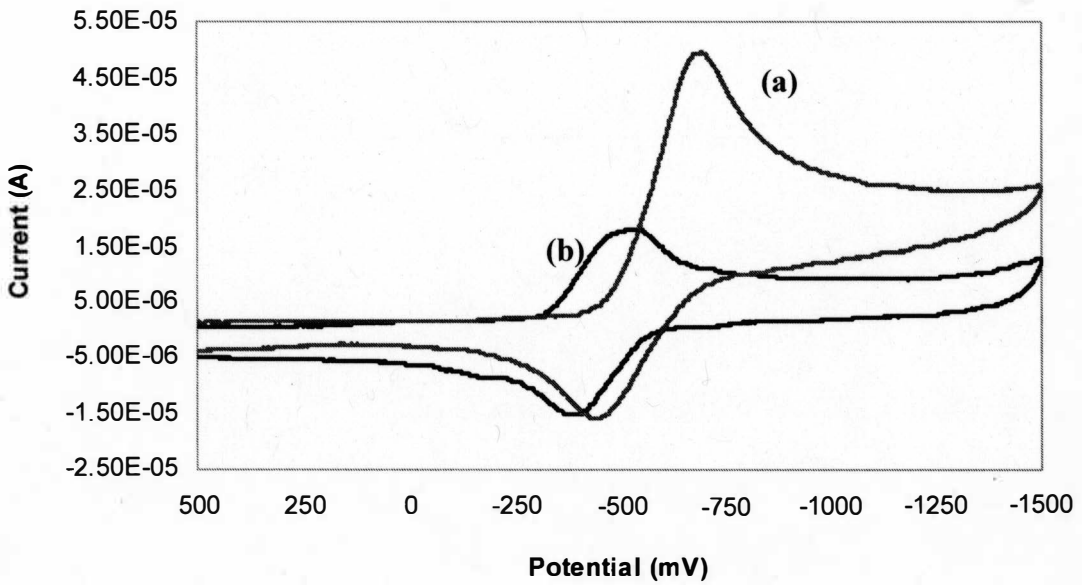

Figure 2.18 Cyclic voltammogram of FMN in different electrolyte solutions (a) in 0.1 M $TBAPF_6/CH_3OH$, (b) in 0.1 M $NaCl/H_2O$. Scan rate = 100 mV/s

Formal potential of FMN was calculated in both solutions. In methanol, $E^{o\prime}$= -562.8 mV vs. Ag/AgCl (3M KCl) whereas in aqueous solution the formal potential was calculated at $E^{o\prime}$= -437.5mV vs. Ag/AgCl (3M KCl). This result is in agreement with the literature value of the corresponding potentials for free FMN where Eq/sq is reported to be -517 mV vs. Ag/AgCl (3.5 M KCl) [16].

Based on this experimental data, the more negative the formal potential, the stronger the reduction capabilities of the system. In this case, in methanol solvent FMN has a stronger reducing capability compared to FMN in aqueous solution. In aqueous solution, FMN is only capable of storing a single electron following photoreduction, thus attributes to lesser capability to reduce TCE.

2.4 Conclusions

Reduction of organohalides are presently of great interest, primarily because of their potential use in the treatment of halogenated solvent wastes as well as in remediation approaches to remove such chemicals from contaminated soils and aquifers. The result of this study has suggested that the reduction of trichloroethylene was observed in the presence of molecular catalysts, $FMNH_2$. The $FMNH_2$ generated from the full reduction of FMN in methanol solvent, which carries two-electrons, has shown reactivity towards TCE reduction.

Different reactivity towards trichloroethylene was observed in aqueous solution. In aqueous solution a semiquinone radical FMNH· is formed. This semiquinone radical only carries one-electron and does not show reactivity towards TCE. This result was

further supported by an electrochemical study which shows that the reduction potentials for FMN in methanol solvent is more negative compared to aqueous solution. The more negative the formal reduction potentials, the stronger the catalysts are for the reduction of trichloroethylene.

In this study, we have observed the importance of modulating the amount of photo-driven generation of electrons towards the reduction of organohalides, in particular for the remediation of trichloroethylene.

2.5 References

1. Mansuy, D., M. Lange, and J.C. Chottard, Reaction of 2,2-bis(p-chlorophenyl)-1,1,1-trichloroethane (DDT) with iron (II) porphyrins. Isolation of the vinylidene carbene complex, tetraphenylporphyriniron (II). Journal of the American Chemical Society, **1978**. *100*: p. 3213-3214.

2. Fukuzumi, S. and J. Maruta, Electron transfer reduction of cobalt tetraphenylporphyrin by hydroquinone dianions and alkylation with alkyl halides. Inorganica Chimica Acta, **1994**. *226(1-2)*: p. 145-150.

3. Glod, G., Angst, W., Holiger, C., Schwarzenbach, R.P., Corrinoid-Mediated Reduction of Tetrachloroethylene, Trichloroethylene, and Trichlorofluoroethene in Homogeneous Aqueous Solution: Reaction Kinetics and Reaction Mechanisms. Environmental Science and Technology, **1997**. *31*: p. 253-260.

4. Holliger, C., Schraa, G., Stams., A.J.M., and Zehnder, A.J.B., Appl. Environ. Microbiol., **1993**. *59*: p. 2991-2997.

5. Neumann, A., H. Scholz-Muramatsu, and G. Diekert, Arch. Microbiology, **1994**. *162*: p. 276-281.

6. Finn, R.D., Basran, J., Roitel, O., Wolf, C.R., Munro, A., Paine, M.J., and Scrutton, N.S., Determination of the redox potentials and electron transfer properties of the FAD- and FMN-binding domains of the human oxidoreductase NR1. European Journal of Biochemistry, **2003**. *270*: p. 1164-1175.

7. Oprian, D.D. and M.J. Coon, Oxidation-Reduction States of FMN and FAD in NADPH-Cytochrome P-450 Reductase during Reduction by NADPH. The Journal of Biological Chemistry, **1982**. *257*(15): p. 8395.

8. Costentine, C., M. Robert, and J.M. Saveant, Does catalysis of reductive dechlorination of tetra- and trichloroethylenes by vitamin B12 and corrinoid-based dehalogenases follow an electron transfer mechanism. Journal of the American Chemical Society, **2005**. *127*: p. 12154-12155.

9. Shey, J. and W.A. van der Donk, Mechanistic Studies on the Vitamin B12-Catalyzed Dechlorination of Chlorinated Alkenes. Journal of the American Chemical Society, **2000**. *122*: p. 12403-12404.

10. Massey, V., The Chemical and Biological Versatility of Riboflavin. Biochemical Society Transaction, **2000**. *28(4)*.

11. Hemmerich, P. and J. Lauterwein, *Inorganic Biochemistry*. The Structure and Reactivity of Flavin-Metal Complex, ed. G.L. Eichhorn. Vol. 1. **1975**, New York: Elsevier.

12. Beinert, H., Spectral Characteristics of Flavins at the Semiquinoid Oxidation Level. Journal of the American Chemical Society, **1956**. *78*: p. 5323-5327.

13. Walsh, C., Flavin Coenzymes: At the Crossroads of Biological Redox Chemistry. Account of Chemical Research, **1980**. *13*: p. 148-155.

14. Borijov Janik, P.J.E., Polarography of Purine and Pyrimidine Nucleosides and Nucleotides. Chemical Review, **1968**. *68*: p. 295-319.

15. Muller, F., Topics in Current Chemistry, **1983**. Vol. *108*. Berlin: Springer-Verlag. p. 71-108.

16. Mayhew, S.G., The effects of pH and semiquinone formation on the oxidation-reduction potentials of flavin mononucleotide. European Journal of Biochemistry, **1999**. *265*. p.698-702

17. Yeni Astuti, E.T., Paul B. Briscoe, Andrea Fantuzzi, Gianfranco Gilardi, James R. Durrant, Proton-Coupled Electron Transfer of Flavodoxin Immobilized on Nanostructured Tin Oxide Electrodes: Thermodynamics versus Kinetics Control of Protein Redox Function. Journal of the American Chemical Society, **2004**. *126*: p. 8001.

18. Voet, D. and J.G. Voet, Biochemistry. 3rd Ed. John Wiley & Sons, Inc.

19. Palfey, B.A. and V. Massey, Comprehensive Biological Catalysis. A Mechanistic Reference. Radical Reactions and Oxidation/Reduction, ed. M. Sinnott. Vol. 3. 1997, San Diego, CA: Academic Press. 83.

20. Edmondson, D.E. and G. Tollin, Semiquinone formation in flavo- and metalloflavoproteins. Top. Current Chemistry, **1983**. *108*: p. 109-138.

21. Ghisla, S., Massey, V., Lhoste, J.M., and Mayhew, S.G., Fluorescence and Optical Characteristics of Reduced Flavines and Flavoproteins. Biochemistry, **1974**. *13(3)*: p. 589-597.

22. Muller, F., Brustlein, M., Hemmerich, P., Massey, V., and Walker, W.H., Light-Absorption Studies of Neutral Flavin Radicals. European Journal of Biochemistry, **1972**. *25:* p. 573-580.

23. Niemz, A. and V.M. Rotello, From Enzyme to Molecular Device. Exploring the Interdependence of Redox and Molecular Recognition. Accounts of Chemical. Research, **1999**. *32*: p. 44-52.

24. Mori, Y. and K. Murata, Vitamins, **1949**. *2*: p. 24.

25. Lowe, H.J. and W.M. Clark, Oxidation-Reduction Potentials of Flavin Adenine Dinucleotide. **1956**. 221(2): p. 983-992.

26. Hasford, J.J., W. Kemnitzer, and C.J. Rizzo, Conformational Effects on Flavin Redox Chemistry. Journal of Organic Chemistry, **1997.** *62*: p. 5244-5245.

27. Yves-Marie Legrand, M.G., Graeme Cooke, Vincent M. Rotello, Model systems for Flavoenzymes Activity: Relationships between Cofactor Structure, Binding, and Redox Properties. Journal of the American Chemical Society, **2003**. *125(51)*: p. 15789-15795.

28. Obare, S.O. and G.J. Meyer, Nanostructured materials for environmental remediation of organic contaminants in water. Journal of Environmental Science and Health A, **2004**. *39(10)*: p. 2549-2582.

29. Obare, S.O., T. Ito, M. Balfour and G.J. Meyer., Ferrous Hemin Oxidation by Organic Halides at Nanocrystalline TiO_2 Interfacess. Nano Letters, **2003**. *3(8)*: p. 1151-1153.

30. Obare, S.O., T. Ito, and G.J. Meyer, Controlling Reduction Potentials of Semiconductor-Supported Molecular Catalysts for Environmental Remediation of Organohalide Pollutants. Environmental Science and Technology, **2005**. *39*: p. 6266-6272.

31. Totten, L.A. and A.L. Roberts, Calculated one- and two-electron reduction potentials and related molecular descriptors for reduction of alkyl and vinyl halides in water. Critical Review Environmental Science and Technology, **2001**. *31*: p. 175-221.

32. Costentine, C., M. Robert, and J.M. Saveant, Succesive removal of chloride ions from organic polychloride pollutants. Mechanism of reductive electrochemical elimination in aliphatic gem-polychlorides. Journal of the American Chemical Society, **2003**. *125*: p. 10729-10739.

33. Sun, M., T.A. Moore, and P.S. Song, Molecular Luminescence Studies of Flavins. I. The Excited States of Flavins. Journal of the American Chemical Society, **1972**. *94*: p. 1730-1735.

34. Muller, F., Topics in Current Chemistry, 1981. **108**: p. 71-108.

35. Dubourdieu, M., J.L. Gall, and V. Favaudon, Biochimica et Biophysica Acta, **1975**. *376*: p. 519-532.

36. Jencks, W.P., Catalysis in Chemistry and Enzymology. Donor-acceptor and charge transfer interaction. **1969**, New York: McGraw Hill.

37. Kuhn, R. and T. Wagner-Jauregg, Ber, **1934**. *67*: p. 361.

38. Michaelis, L., M.P. Schubert, and C.V. Smythe, The Journal of Biological Chemistry, **1936**. *116*: p. 587.

39. Michaelis, L. and G. Schwarzenbach, Ibid, **1938**. *123*: p. 527.

40. J. Woodland Hastings and Quentin H. Gibson., Intermediates in the Bioluminescent Oxidation of Reduced Flavin Mononucleotide. The Journal of Biological Chemistry, **1963**. *238(7)*: p. 2537-2554.

41. Flowers, P.A. and S.-A. Callender, Variable Path Length Transmittance Cell for Ultraviolet, Visible and Infrared Spectroscopy and Spectroelectrochemistry. Analytical Chemistry, **1996.** *68*: p. 199-202.

42. Swinehart, J.H., Electron Transfer in the Flavin Mononucleotide System. Journal of the American Chemical Society, **1966**. *88(5)*: p. 1056-1058.

43. Swinehart, J.H., Kinetics of the Flavin Mononucleotide System. Journal of the American Chemical Society, **1965**. *87(4)*.

44. S. H. Song, B.D., A. Penzkofer, P. Hegemann, Photo-reduction of flavin mononucleotide to semiquinone form in LOV domain mutants of blue light receptor phot from Chlamydomonas reinhardtii. Journal of Photochemistry and Photobiology B: Biology, **2007**. *87*: p. 37-48.

45. Muller, F., Chemistry and Biochemistry of Flavoenzymes. Vol. 1. **1991**, Boca Raton: CRC Press.

46. Barman, B.G. and G. Tollin, Kinetics and Equlibria in Partially Reduced Flavine Solutions. Biochemistry, **1972**. *25:* p. 4760-4765.

47. Land, E.J. and A.J. Swallow, One-electron reactions in biochemical systems as studied by pulse radiolysis. Biochemistry, **1966**. *8*: p. 2117-2125.

CHAPTER III

ANCHORING FLAVIN MONONUCLEOTIDE ONTO NANOCRYSTALLINE TIO_2 SURFACES

3.1 Introduction

3.1.1 Catalysis in Aqueous Solution

It is always desirable to find environmentally acceptable reagents that effect desired specific chemical transformation, but at the same time avoid unneeded byproducts and certain solvents (such as organic solvents). From the discussion in Chapter II of this thesis, it was clearly shown that there is a difference in reactivity of FMN towards trichloroethylene (TCE) in aqueous vs. organic solvents. Catalysis in aqueous solution is a promising area of research especially since it avoids the use of chemicals or solvents that add to the overall pollution problem [1-3]. For example, organometallic catalysis in aqueous solution has been successfully performed by Espenson et al, in which the catalysis of the oxidation of bromide ions by hydrogen peroxide is efficiently carried out by methylrhenium trioxide [2].

Recent research by Thomas Mallouk and coworkers has focused on the development of methods for destruction of chlorinated organic molecules, such as CCl_4, PCE and TCE, in ground water and surface waters [4]. They have reported successful dehalogenation of TCE using high-surface area nickel-iron nanoparticles (1:3 Ni :Fe), in aqueous media where TCE concentration was reduced from 24 ppm to <6 ppb in 120 minutes [4]. Yet, there are some problems associated with this method such as (1)

formation of toxic byproducts namely *cis*-dichloethylene (DCE) and vinyl chloride (VC), and (2) limited lifetime of zero-valent metal nanoparticles due to corrosion.

3.1.2 Multi-Electron Transfer

Multi-electron transfer systems (MET) are attracting interest for a variety of applications including environmental remediation, electrochromic displays, and photoelectrochemical energy conversion [5]. MET is a process of electron transfer that involves multiple electrons being generated, trapped and transferred to a desired compound to yield a specific chemical transformation. The advantage of using MET processes over single-electron transfer (SET) systems is to eliminate high-energy free radical intermediates and to produce desired reaction products under mild and environmentally relevant conditions.

Surprisingly, there are only a few clear examples of MET that can be found in the literature [6-9]. The biggest challenge for MET research is to synthesize molecular compounds or materials capable of storing and transferring multiple electrons, although some groups have been successful. Nocera reported the reactivity of iron porphyrinogens actively participates in redox chemistry via discrete two-electron steps by storing multi-electron equivalents [31]. Stromberg et al recently reported a new design for a MET system consisting of a molecular catalyst heme functionalized onto nanocrystalline TiO_2 for the reductive dechlorination of dichloro-diphenyl-trichloroethane (DDT) and tetrachloroethylene (CCl_4) [10]. Obare and Meyer reported the reduction of organic halides by ferrous hemin anchored to nanocrystalline TiO_2 thin films, in which the

ferrous state was generated through band gap illumination of the hemin-modified semiconductor [11].

Synthesis of nanomaterials capable of harvesting solar energy and storing multiple electrons are advantageous toward the development of MET systems. In general, MET systems allow access to specific reaction transformations by avoiding high-energy free radical intermediates and can yield reaction products under mild, environmentally relevant reaction conditions [6, 10]. However, in comparison to molecular catalysts, nanomaterials or solid-state materials often lack the selectivity offered by molecular systems. Nonetheless, recent reports of molecular catalysts covalently bound to mesoporous nanoscale semiconductor materials have shown some success in environmental remediation processes [11, 12]. In this case, the semiconductor nanoparticles used as solid supports allow the active state of the molecular catalysts to be maintained either photochemically or electrochemically in the environment. Recently, Obare et al initiated experiments with molecular catalysts bound to nanocrystalline semiconductor surfaces [11, 12]. These materials were investigated for organohalide pollutant reduction.

3.1.3 Functionalization of FMN/TiO_2

Titanium dioxide has been widely used as a pigment, in sunscreens, paints, ointments, and toothpaste. Titanium dioxide is chemically stable, relatively hard, non-toxic, bio-compatible, largely transparent and inexpensive. TiO_2 occurs in 3 crystalline forms: anatase, rutile and brookite. Degussa-P25 is the commercially available TiO_2

which is composed of 80% anatase and 20% rutile. Anatase is a wide band-gap semiconductor (3.2 eV) with a large range of electrical conductivity depending on its chemical composition. In general, anatase has been considered the most photochemically active phase of TiO_2 due to a higher surface adsorptive capacity towards many organic compounds, while the rutile phase is generally less active because of higher rates of recombination of the photogenerated charge carriers [13].

These properties of titanium dioxide have resulted in an increased interest in its use for various applications including photovoltaics, photocatalysis, photo-electrochromics and sensors [14]. Since the early 1970s, mesoporous anatase TiO_2 thin films coated with dyes find use as photoanodes of photoelectrochemical cells for solar energy conversion. Interest in this field has exponentially increased in the last decade, since Grätzel and coworkers produced the first cells with substantially higher conversion efficiencies by using sol-gel techniques to manufacture films with enormous surface area for the dye uptake [14]. This cell, commonly called Dye Sensitized Solar Cell (DSSC) or Grätzel cell was first designed by Michael Grätzel in 1991.

Photocatalysis using titanium dioxide has been considered the most important and new, environmentally friendly, clean chemical technology for green chemistry. In principle, various applications of titanium dioxide photocatalysts have already been developed to address environmental decontamination of various pollutants [1, 7, 10, 12, 13, 15-17]. This method has been successful in the purification of the polluted atmospheres as well as toxic water using ultraviolet light having a wavelength shorter than 380 nm (a larger energy than the band gap of the titanium dioxide photocatalysts). The design and development of such unique titanium dioxide photocatalysts can be

considered a breakthrough in the efficient and large-scale utilization of solar energy. However, a major limitation associated with TiO_2 photocatalysis, is high rate of charge recombination between the photogenerated holes and electrons [18].

Galoppini, has shown that molecular compounds including dyes can be anchored to metal oxides via phosphonic acids ($P(O)OH_2$), carboxylic acids (COOH) and their derivatives such as esters, acid chlorides, carboxylate salts, or amides [19]. Silanes (SiX_3), ethers, acetylacetonate and salicylates have also been used. The strong binding with metal oxides occurs through the reaction with the surface hydroxyl groups [19]. These groups are the best for anchoring to the surface of metal oxide due to the hard-hard acid-base theory, where hard acids such as carboxylic acids and phosphonic acids will prefer strong binding to hard bases such metal oxides. Chemisorption at TiO_2 surfaces via COOH groups can occur through a variety of binding modes [12] and the prevalent mode is dependent on the structure of the molecule being anchored, the binding groups, the pH of the semiconductor surface.

As mentioned in the previous chapter, FMN possesses a phosphonic acid functional group that can bind to the hydroxyl group on the surface of nanocrystalline TiO_2 thin films as shown in Figure 3.1.

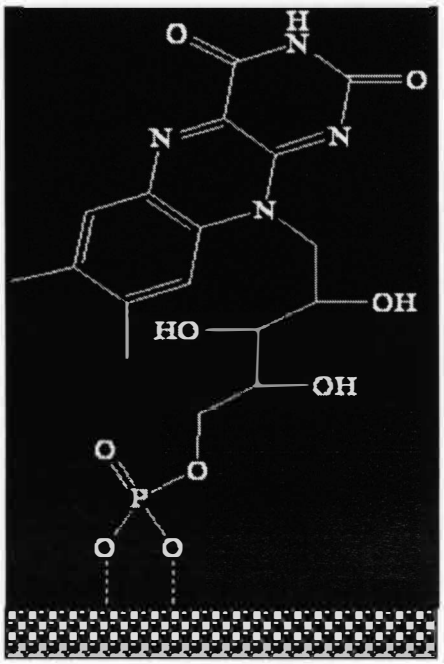

Figure 3.1 Anchoring FMN onto the surface of nanocrystalline TiO_2 thin film via phosphonic acid interaction with metal oxide (not drawn to scale)

FMN anchored on the surface of nanocrystalline TiO_2 thin films were found to trap, store and transfer multiple electrons to trichloroethylene (TCE). The advantage of anchoring FMN on the surface of nanocrystalline TiO_2 thin films are as follows: 1) enhances selectivity and catalytic activity for specific chemical transformation, 2) allows recovery of the catalyst since the reactants and catalysts are not in the same phase and 3) allows involvement of the TiO_2 conduction band electrons (e^-_{CB}) generated from irradiation on TiO_2 to promote increased reactivity and allow certain chemical transformations.

Grätzel and Fitzmaurice also reported that nanocrystalline thin films has a large effective surface area and consequently high concentration of surface states [20]. This

enormous surface area of the thin films was afforded by high concentrations of catalysts (approaching one molar within the film) while still at monolayer or lower surface coverage.

The most obvious advantage of nanocrystalline mesoporous TiO_2 thin films over colloidal suspensions is that they can be introduced into and removed from a wide variety of environments including ground and ocean water. In addition, by interconnecting the nanoparticles the mesoporous structure does not suffer from aggregation or "salting out" which is common in colloidal suspensions. According to Barbe et al, the mesoporous structure also allows facile diffusion of RX and other pollutants to the catalytic site on the film [32].

The proposed multi-electron transfer catalyst is shown in Figure 3.2. In scheme a, irradiation of TiO_2 semiconductor promotes an electron from the valence band (VB) to the conduction band (CB). The holes in the valence band react with the solvent to produce the oxidized solvent (solvent*). Electrons are then transferred from the conduction band to the molecular catalyst (FMN) to provide the extra electron. In scheme b, reactive electrons from both TiO_2 semiconductor and molecular catalyst ($FMNH_2$ generated from FMN irradiation) are transferred to substrate (organohalides) and thus reduce the organohalides.

The synthesis and fabrication of the MET catalyst and its reaction towards trichloroethylene will be described in this chapter.

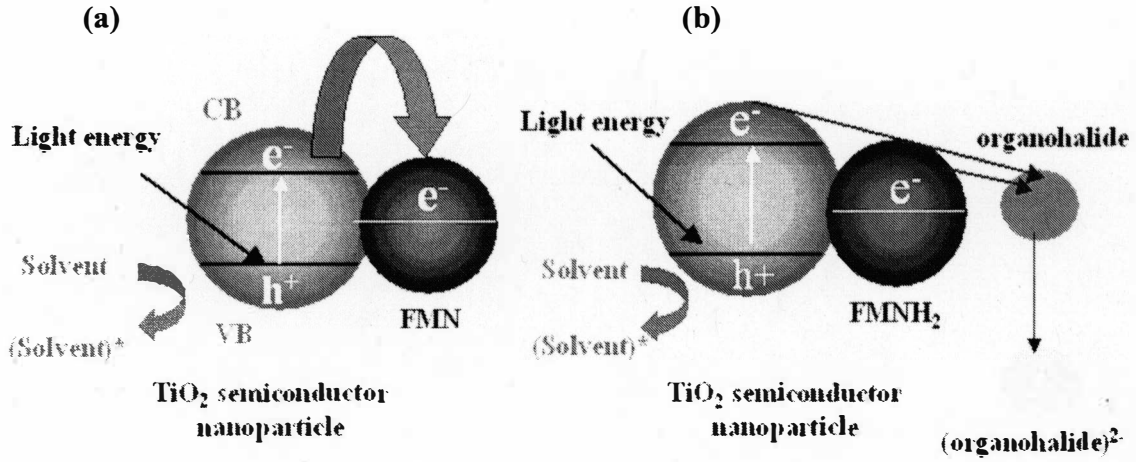

Figure 3.2 Proposed multi-electron transfer catalysis reaction

As more research is geared toward solving current environmental pollution, it is attractive to design a hybrid system that promotes catalysis reaction in various conditions, yet still specific to a certain chemical transformation. Herein, the hybrid catalyst consists of inorganic-organic molecules of FMN/TiO_2 and it promotes the catalysis reaction of organohalides not only in organic solvents but also allows reactions to be carried under aqueous solution to promote green chemistry. The elucidation of multi-electron transfer (MET) reactivity at TiO_2 nanocrystalline semiconductor interfaces under aqueous media will be discussed. In addition, the study of multi-electron transfer of FMN/TiO_2 hybrid catalyst towards TCE degradation will be discussed. Furthermore, the reduction of TCE with an assembly of a system that can deliver multiple electrons will be discussed in great details. In this research, a well-defined molecular catalyst (FMN) is anchored to

mesoporous nanocrystalline anatase TiO_2 thin films. Meyer has reported earlier that MET catalysts was generated by functionalization of TiO_2 surface with molecular catalysts[10, 11]. The method that we develop in this research is unique because it was found that the reductive dechlorination reaction could be carried not only in organic solvent (methanol solution) but also in aqueous solution. By carrying transformation in aqueous solution, the elimination of toxic byproducts from the reactions becomes more plausible.

3.2 Experimental Section

3.2.1 Materials and Reagents

Riboflavin 5'-monophosphate sodium salt dihydrate (FMN), Titanium (IV) isopropoxide ($Ti(iOPr)_4$), methanol (CH_3OH) ≥99%, trichloroethylene (anhydrous) ≥99%, and tetrabutylammonium hexafluorophosphate ($TBAPF_6$) were obtained from Sigma Aldrich. Anhydrous methanol was prepared by soaking molecular sieves in the methanol solution ±60 minutes and used as prepared. Deionized Milli-Q water at a pH of ~7 was used where aqueous measurements are described. Concentrated HNO_3 (ACS grade) was obtained from Fischer. Standard quartz cuvette with 1 cm path length was used for all UV-visible absorbance measurements. Aqua regia (3:1 v/v HCl: HNO_3) was used to clean all glassware prior of use. The reduction of TCE was measured in either methanol or in water. In the case of methanol, 0.01 M solution of TCE in methanol was prepared and used. For aqueous experiments, due to low solubility of TCE in water (1

g/L of water at 20 C), 5 mL of TCE was stirred overnight in 20 mL of aqueous solution. The aqueous solution containing saturated TCE was used for subsequent measurements.

Hamilton syringes (500 μL and 250 μL) and microscope glass slides were obtained from VWR International (3 in x 1 in, 1 mm). Barnstead Thermolyne 1300 Furnace was used to prepare TiO_2. Indium-doped Tin Oxide (ITO) "conductive glass" slide was purchased from Hartford Glass Company, Inc.

3.2.2 Instrumentation

UV-visible absorbance spectra were acquired using a Varian Cary 50 UV-visible spectrophotometer. Fluorescence measurements were obtained using and Varian Cary Eclipse Spectrofluorometer. Irradiation was carried out using a 400W Xe lamp, and 21.7 kA with a KV 370 (370 nm cutoff) filter From Newport, Inc. In each case, samples were irradiated for 30 minutes. All experiments were carried out under a nitrogen atmosphere, by purging all solutions with ultra high pure compressed N_2 (Airgas, inc).

3.2.3 Nanocrystalline TiO_2 Film Preparation

Transparent TiO_2 films consisting of ~10-12 nm diameter anatase particles were prepared by the hydrolysis of $Ti(iOPr)_4$ using a sol-gel technique as previously described in the literature [21]. Titanium (IV) isopropoxide was used as a precursor in acid-catalyzed hydrolysis reaction as follows:

$$Ti(OR)_4 + 2H_2O \rightarrow TiO_2 + 4\ ROH$$

3.2.4 Fabrication of FMN/TiO_2 Thin Film Slide

TiO_2 paste was cast as mesoporous thin (~10 μm) films onto microscope glass slides or transparent indium-doped tin oxide (ITO). The attachment of FMN to the TiO_2 surface was achieved by soaking freshly prepared TiO_2 films in a 1.0 x 10^{-4} M FMN solution in methanol for ± 24 hours. The concentration of FMN adsorbed on the TiO_2 surface was determined by calculating the difference of the concentration of FMN before and after TiO_2 soaking. Once FMN was anchored, it remained strongly bound to the surface in both methanol and aqueous solutions.

The nanocrystalline thin films were placed diagonally in a standard quartz cuvette. Absorption spectra and steady-state kinetic measurements were acquired using a Cary 50 UV-visible absorbance spectrophotometer. Irradiations of FMN/TiO_2 films or FMN in solution were carried out using a 1000-W Xe lamp with a KV 370 filter. In each case, samples were illuminated for 30 min at 400W.

3.2.5 Atomic Force Microscopy

Colloidal TiO_2 nanoparticles were imaged on a PicoPlus Atomic Force Microscope instrument (AFM) purchased from Molecular Imaging, Inc. Sample preparation for AFM image was done as follows: 2 μL of diluted TiO_2 nanoparticles were drop-cast on a Highly Oriented Pyrolytic Graphite (HOPG) conductive substrate which was attached to a cover slip using a double-sided tape. The sample was air-dried for three hours prior to imaging. The image was obtained in a vibration free box, operated on non-contact Acoustic AC (AAC) mode, and using AFM tip attached on the cantilever. Images

were recorded using either the AFM "M" piezo scanner with a maximum scan range of 2.5 μm x 2.5μm. Topographical AFM image was collected in deflection mode.

3.2.6 Electrochemistry/ Surface Spectroelectrochemistry

Sweep Mode Cyclic Voltammetry was conducted using a CV 50W Potentiostat (BAS Bioanalytical System, Inc), consisting of three-cell arrangement consisting of a Pt gauze counterelectrode, a glassy carbon working electrode and Ag/AgCl (3 M KCl) reference electrode. For supporting electrolytes, 0.1 M tetrabutylammonium hexafluorophosphate ($TBAPF_6$) was used. The sample was placed in an electrochemical cell compartment pre-washed with aqua regia prior to use. Purging for 10 minutes with ultra high pure nitrogen gas took place prior to each measurement. A blank run was taken prior to sample analysis. Cyclic voltammograms were recorded at scan rates of 100 mV/s.

For TiO_2 surface studies, the TiO_2 pastes were cast as mesoporous thin (~10 μm) films onto transparent indium-doped tin oxide (ITO) glass slides and used as the working electrode. The attachment of FMN to the TiO_2 surface was achieved by soaking freshly prepared ITO/TiO_2 films for at least 12 hours in a 1.0 x 10^{-4} M FMN solution in methanol. A custom-designed quartz cuvette with a 1 cm path length was used as the spectroelectrochemical cell with solvent volume of 10-15 mL. Spectroelectrochemical measurements were conducted on CV 50W Potentiostat to apply the desired potentials in a standard three-electrode arrangement with a Pt counterelectrode, Ag/AgCl (3 M KCl) reference electrode, and ITO/TiO_2/FMN as a working electrode on alligator clips. N_2 atmosphere was kept throughout the measurements by bubbling nitrogen to the solution. A fresh solution of 0.1 M tetrabutylammonium hexafluorophosphate ($TBAPF_6$) in

acetonitrile was used as the supporting electrolyte. A Ag/AgCl (3M KCl) purchased from Bioanalytical Systems Inc. was used as the reference electrode. The inner element is a silver wire immersed in a solution of $AgCl_{sat}$/KCl (3M). A Varian Cary 50 UV-visible absorbance spectrophotometer was used to measure absorbance spectra. Each potential was held until the UV-visible absorbance spectrum became time-independent, and steady state concentrations were assumed.

3.2.7 Steady-State Kinetic Analysis of Trichloroethylene Reactivity

A Varian Cary 50 UV-visible absorbance spectrophotometer was used to acquire time resolved spectra for the reaction of $FMNH_2/TiO_2$ (in aqueous solution) and $FMNH_2/TiO_2(e^-_{CB})$ (in methanol solvent) with TCE. An aliquot of N_2 saturated TCE in MeOH or TCE in H_2O was added to the $FMNH_2/TiO_2(e^-_{CB})$ thin film immersed in either a methanol solvent or an aqueous solution. The appearance of a 445 nm absorbance of FMN and the disappearance of the 700 nm absorbance peak corresponding to $TiO_2(e^-_{CB})$ were monitored by steady-state kinetics. Pseudo-first order kinetic rate, k_{obs} were obtained by fitting to equation 3.1. Analysis was conducted using a scientific graphic and analysis software ORIGIN version 7.5.

$$\ln A = \ln A_0 - k_{obs}\, t \qquad \text{(Eq. 3.1)}$$

Where A = absorbance, A_0 = initial absorbance, t = time, and k_{obs} = observed rate constant

3.2.8 Product Analysis

Products of TCE reduction in $FMNH_2/TiO_2(e^-_{CB})$ were analyzed by GC/MS. An aliquot (1 μL) of sample extracts from methanol solution were analyzed by GC on HP 6890 Series GC System (Hewlett Packard), equipped with a HP 5973 mass selective detector. The sample was kept in a N_2 atmosphere to avoid reactivity with oxygen. Headspace samples were obtained and transferred using 10 μL gastight syringes purchased from Hamilton. The column used was a capillary column (30.0 m x 250 μm x 0.25 μm nominal) purchased from SGE Forte. The parameters for front inlet were set as follows: splitless mode using He carrier gas, heater at 250 °C, 10.5 psi. The GC oven was initially set at 80 °C for 5 min, heated at 8 °C/min to 150 °C and kept for 3 min.

3.3 Results and Discussion

3.3.1 Mesoporous Nanocrystalline TiO_2 Thin Film

Scanning electron micrograph (SEM) image of nanocrystalline TiO_2 thin film that was synthesized with a sol-gel method [21] is shown in Figure 3.3. In a typical sol-gel process, a colloidal suspension, or a sol, is formed from the hydrolysis and polymerization reactions of the titanium precursors. This process normally proceeds via an acid-catalyzed hydrolysis of titanium (IV) alkoxide followed by condensation. The development of Ti-O-Ti chains is favored with low content of water, low hydrolysis rate, and excess titanium alkoxide in the reaction mixture.

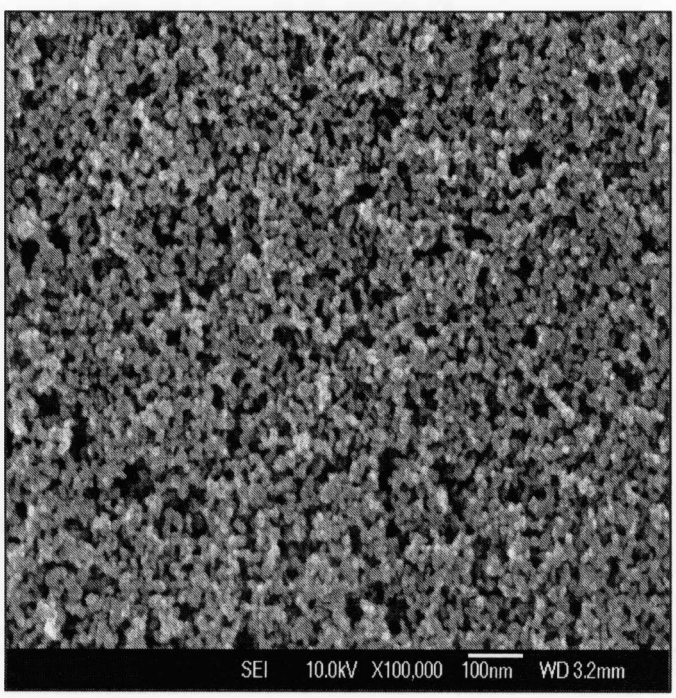

Figure 3.3 SEM image of a colloidal TiO_2 anatase particles imaged using JEOL scanning electron microscope

The as-prepared anatase TiO_2 nanoparticles are transparent in the visible region and have a narrow size distribution of ~10-12 nm. The film has a surface area such that 800 $\pm$ 200 molecules can be anchored to a nanoparticle [11]. This also provides more active site for the reaction with organohalides.

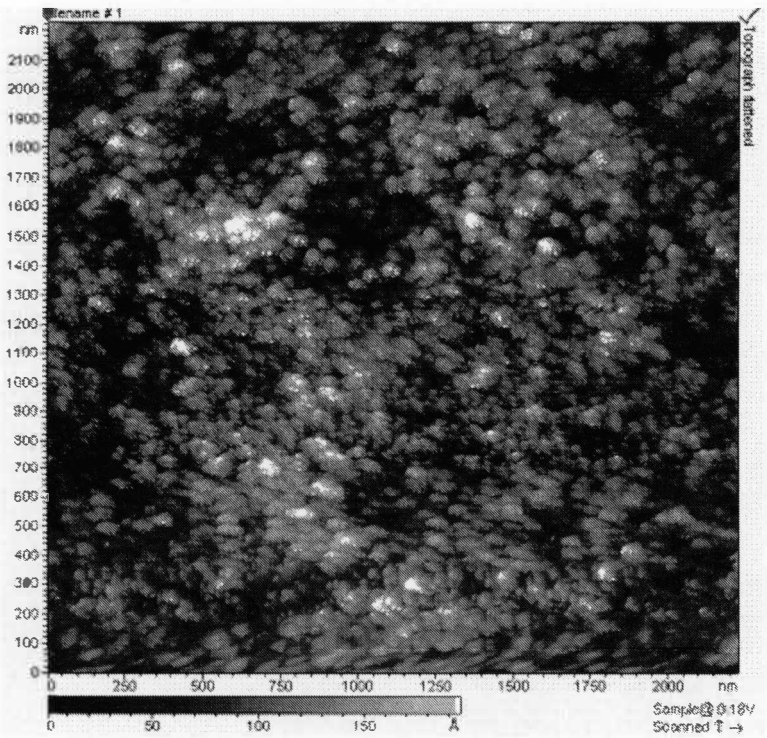

Figure 3.4 Atomic Force Microscope (AFM) image of mesoporous colloidal consisting of ~10 nm diameter TiO_2 anatase particles imaged using PicoPlus AFM Acoustic Alternating Current (AAC) mode on a Highly Oriented Pyrolytic Graphite (HOPG) substrate

3.3.2 Irradiation of TiO_2

When anatase titanium dioxide are irradiated with energy greater than or equal to the band gap energy (~ 3.2 eV), it results in electron-hole pair separation. Electrons are promoted to the conduction band, while the holes remain in the valence band.[22] Excited-state conduction-band electrons and valence-band holes can recombine and dissipate the input energy as heat, get trapped in metastable surface states, or react with electron donors and electron acceptors adsorbed on the semiconductor surface or within the surrounding electrical double layer of the charged particles.

In the presence of a hole scavenger, it is possible to avoid electron-hole recombination and thus allow electron accumulation in the conduction band. In the case of anatase TiO_2 nanoparticles, the accumulation of conduction band electrons is accompanied by an increase in the absorption of TiO_2 in the 400 nm – NIR region and blue coloration. Electrons and holes generated in TiO_2 nanoparticles are localized at different defect sites on the surface and in the bulk. Electron paramagnetic resonance (EPR) results have shown that electrons are trapped as two Ti(III) centers, while the holes are trapped as oxygen-centered radicals covalently linked to surface titanium atoms [22]. Valence band holes are known to irreversibly oxidize methanol to form formaldehyde, thus allowing the concentration of $TiO_2(e^-)$ to build up under steady-state irradiation [6].

$$Ti^{IV}O_2 + e^- + H^+ \longrightarrow Ti^{III}(O)(OH)$$

The blue coloration of TiO_2 colloids has been attributed to the trapping of electrons at the Ti^{4+} sites[14]. This blue coloration of TiO_2 remains unchanged in room

light in an inert atmosphere. The blue coloration will disappear when an electron scavenger such as dissolved oxygen and/or water are introduced to the system. Szczepankiewicz and Hoffmann et al. found that O_2 was an efficient scavenger of conduction band electrons at the gas/solid interfaces and the build-up of trapped carriers eventually resulted in extended surface reconstruction involving Ti-OH functionalities [6]. This blue coloration of TiO_2 colloids is useful in quantifying the number of electrons stored in TiO_2 nanoparticles. The conduction band electrons are highly reactive reductants while the holes are highly reactive oxidants, which together induce catalytic reactions on the catalyst surface, namely photocatalytic reactions. The Irradiation of TiO_2 thin film in methanol solvent is shown in Figure 3.5.

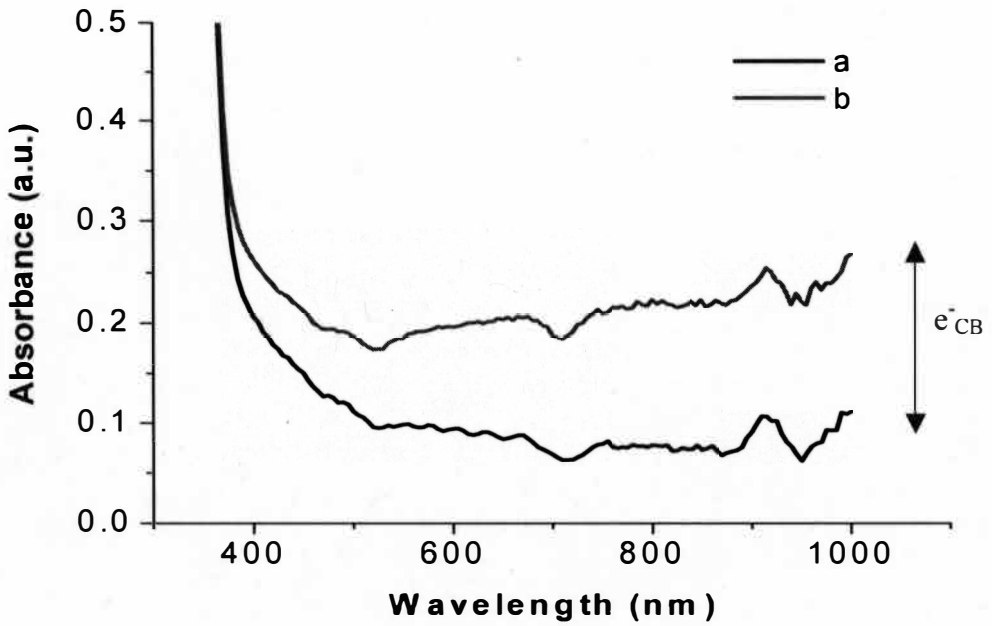

Figure 3.5 UV-visible absorbance spectra of TiO_2 thin-film slide in a deaerated solution of methanol (a) before irradiation, and (b) after irradiation

The UV-visible absorbance spectra of TiO_2 before and after irradiation shows that an increase in the absorbance intensity after 400 nm into the NIR, and the film is accompanied by blue coloration, indicating the accumulation of trapped conduction band electrons (e^-_{CB}). Similar observations have been reported by Grätzel and Highfield [23] who studied the photochromism in Degussa P-25 TiO_2 following band-gap excitation. Fitzmaurice and co-workers have studied the electron accumulation and compensation in nanostructured TiO_2 (anatase) electrodes. They also observed the increased absorbance extending to the near-infrared which was assigned to intra- and interband transitions by electrons occupying the conduction band states [24].

3.3.3 Fabrication of FMN/TiO_2 Interfaces

The schematic for the fabrication of FMN on the surface of TiO_2 is shown in Figure 3.6. This organic-inorganic hybrid catalyst is composed of nanocrystalline TiO_2 thin film functionalized with FMN via phosphonic acid linking group. The attachment of FMN to the nanocrystalline TiO_2 produced a bright-yellow film with a UV-visible absorption spectrum at 445 nm. The concentration of FMN on the surface was calculated to be 4.30×10^{-5} M upon soaking with 10^{-4} M FMN solution overnight. The slide turned from colorless to yellow indicating adsorption of FMN to the surface of TiO_2. FMN anchored to the TiO_2 surface was found to be stable, in both organic and aqueous solutions for periods of days. The concentration of FMN on the surface of TiO_2 was calculated by measuring the difference in concentration of FMN before and after soaking for 24 hours.

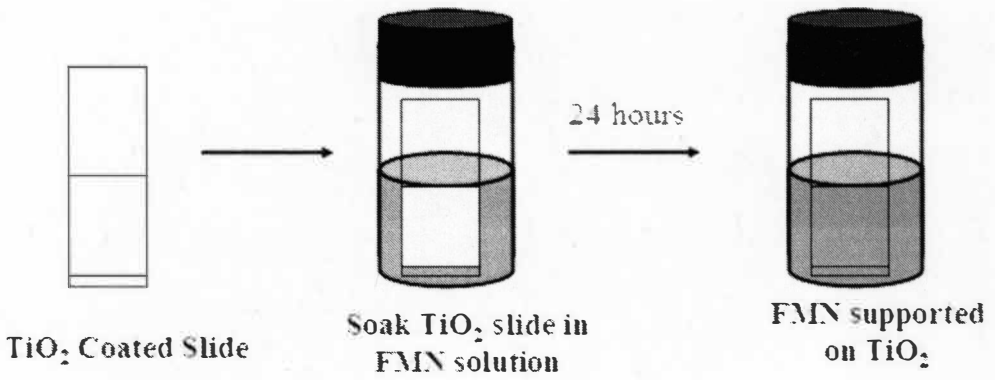

Figure 3.6 Schematic representation of FMN/TiO_2 fabrication on a quartz glass slide

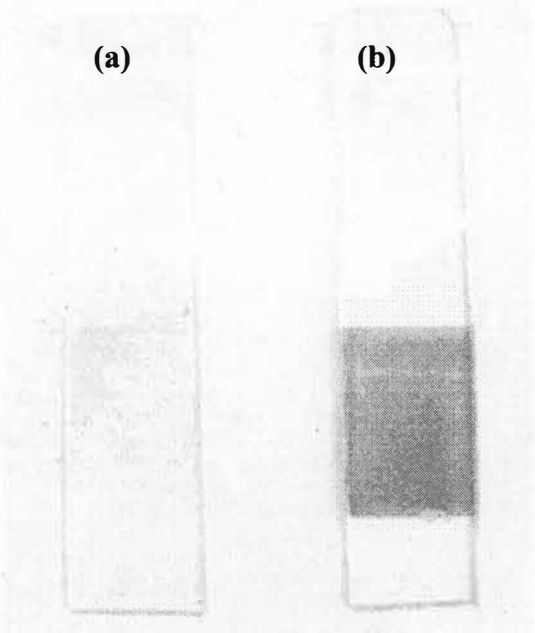

Figure 3.7 Photographs of (a) nanocrystalline TiO_2 coated on a glass slide (b) FMN anchored nanocrystalline TiO_2 on a glass slide

3.3.4 Reactivity of $FMNH_2/TiO_2$ Towards Trichloroethylene in Aqueous Solution

The reactivity of $FMNH_2/TiO_2$ with trichloroethylene was analyzed. As mentioned earlier, band gap excitation produces an electron-hole pair. Band gap irradiation (λ < 370 nm) of FMN/TiO_2 in aqueous solution was found to yield $FMNH_2/TiO_2$. In this case, the conduction band electrons (e^-_{CB}) contribute to the reduction of FMN to $FMNH_2$ but due to the high rate of TiO_2 electron-hole recombination in aqueous solution, no electrons accumulate in the conduction band. Part of the explanation of this is due to different energetic of conduction band energies for nanocrystalline TiO_2 when they are in contact with aqueous electrolytes [25].

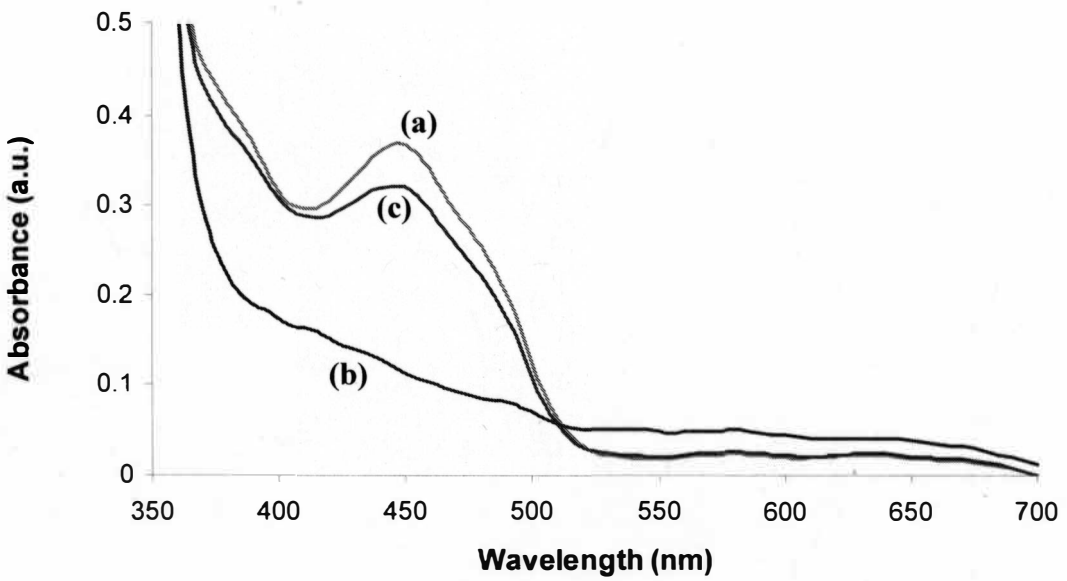

Figure 3.8 UV-visible absorbance spectra of $FMNH_2/TiO_2$ in aqueous solution: (a) before irradiation, (b) after irradiation and (c) after addition of TCE in the *dark*

FMN bound to the TiO_2 surface showed an absorbance maximum peak at 445 nm (E_g = 3.2 eV). Following TiO_2 band gap irradiation, FMN undergoes complete photoreduction to $FMNH_2$, which is displayed by the disappearance of 445 nm peak maxima. Addition of trichloroethylene in the *dark* was found to generate the initial FMN/TiO_2 absorption spectrum as seen on Figure 3.8.

The fluorescence spectrum of FMN anchored on TiO_2 on Figure 3.9 shows a peak maximum at 525 nm, corresponding to the emission wavelength of FMN. Following irradiation, FMN is completely reduced to $FMNH_2$ characterized by the loss of emission maximum. Addition of TCE in the *dark* resulted in the re-oxidation of $FMNH_2$ to FMN (reappearance of 525 nm peak) and reduction of TCE. This result confirmed that the reduction of TCE occurs using the hybrid catalyst of $FMNH_2/TiO_2$ in aqueous solution.

A proposed mechanism for the FMN photoreduction is similar for molecular compounds on TiO_2 interfaces [26, 27], whereby band gap excitation produces an electron-hole pair, and the conduction band electron (e^-_{CB}) acts as a reductant that reduces FMN to $FMNH_2$. The above results demonstrate organohalide reduction in an aqueous solution, which is promising as it shows the ability to degrade pollutants under conditions that mimic the environment.

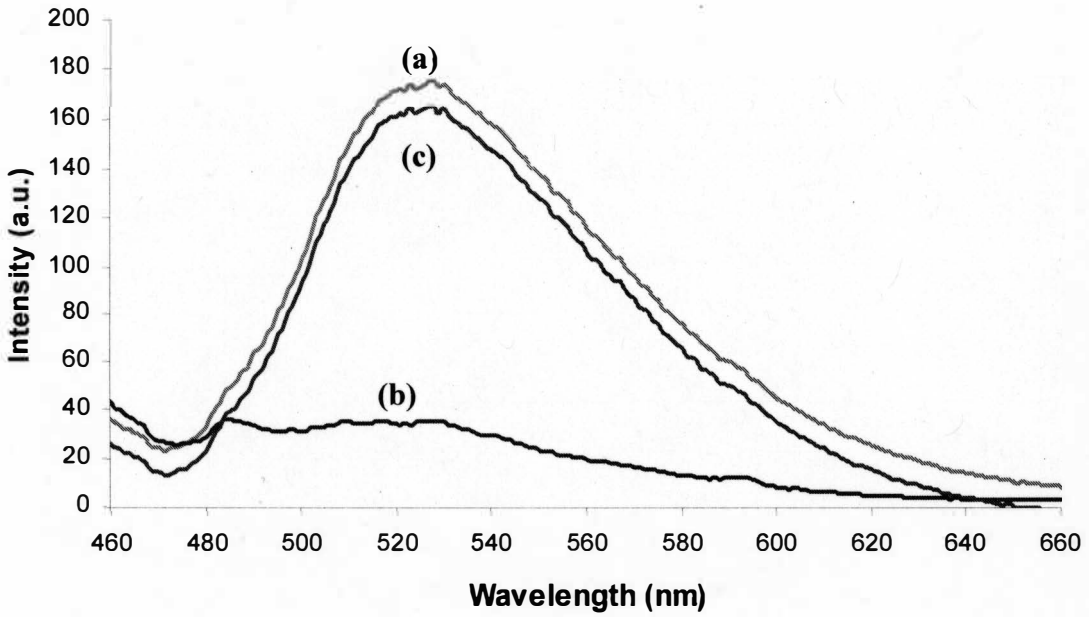

Figure 3.9 Fluorescence spectra of $FMNH_2/TiO_2$ in aqueous solution and its reactivity towards TCE (a) before irradiation, (b) after irradiation and (c) after addition of TCE in the *dark*

The reduction rate constant of TCE by $FMNH_2/TiO_2$ is calculated via measuring the change in absorbance *vs*. time upon addition of TCE to the system. The results are shown in Figure 3.10.

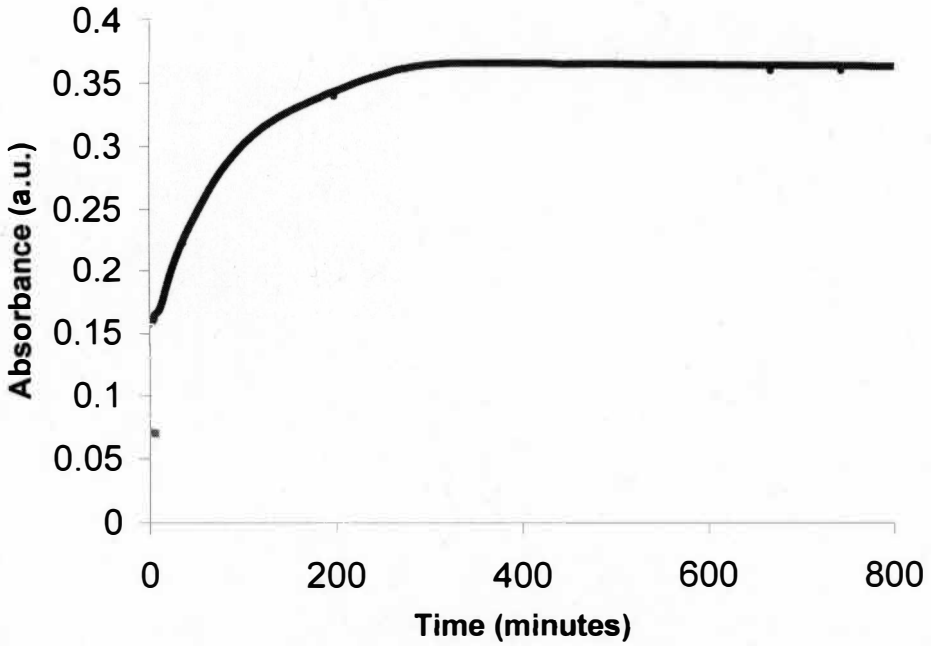

Figure 3.10 Time resolved absorption changes monitored at 445 nm following the addition of TCE in the *dark*

Injection of saturated TCE in water resulted in the oxidation of $FMNH_2$ to FMN where the 445 nm absorbance intensity increased as a function of time, and then reached steady state at ~0.37 a.u. corresponding to the oxidation of $FMNH_2$ to FMN. This was accompanied by the reduction of TCE. Comparative studies with titanium dioxide electrons in the absence of FMN were also investigated for a control experiment where the $TiO_2(e^-)$ showed no reactivity towards TCE monitored at 5 hours after the addition of TCE as seen on Figure 3.11 and Figure 3.12.

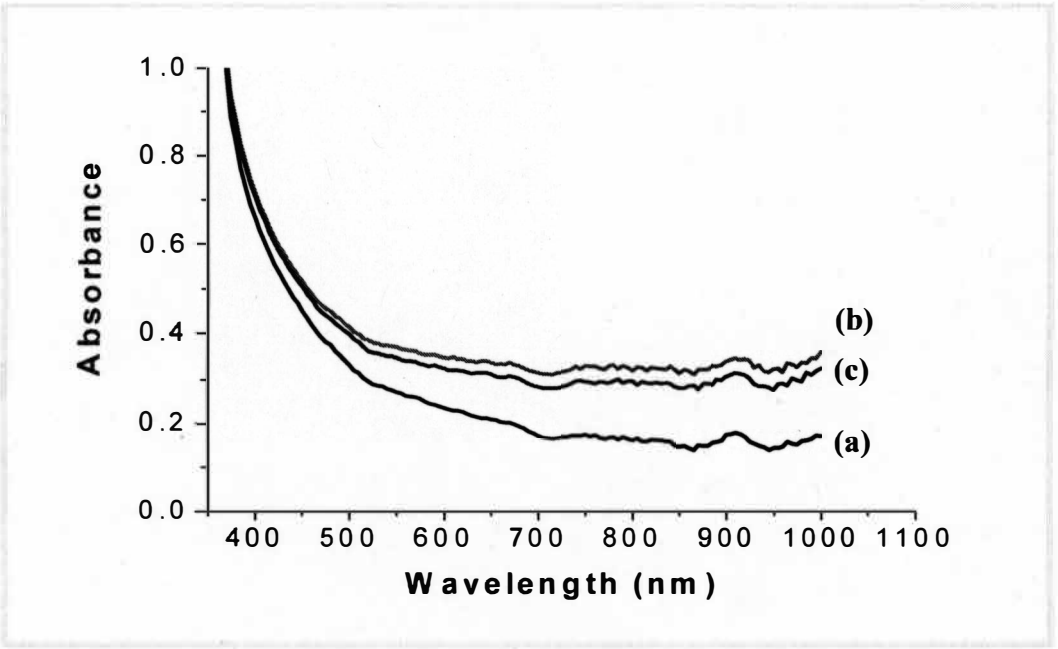

Figure 3.11 Reaction of $TiO_2(e^-_{CB})$ with TCE a) before irradiation, b) after irradiation, and c) after addition of TCE in the *dark* (t = 5 hours)

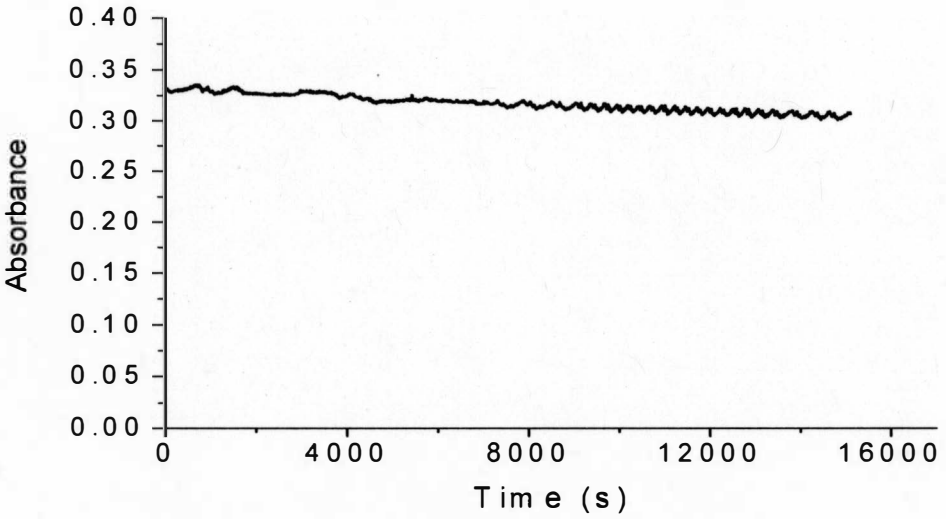

Figure 3.12 Time absorption changes of $TiO_2(e^-_{CB})$ with TCE addition in the *dark*

Observed rate constant (k_{obs}) were abstracted from the absorption changes for the disappearance of FMN/TiO_2 and the appearance of $FMNH_2/TiO_2$. Figure 3.13 showed plot of k_{obs} vs. concentration of TCE in aqueous solution. Pseudo-first order kinetic rate constant, k_{obs} were obtained by fitting to equation 3.10. In this particular system, the reduction rate constant k of TCE is calculated to be 2.6 M^{-1} s^{-1} in aqueous solution.

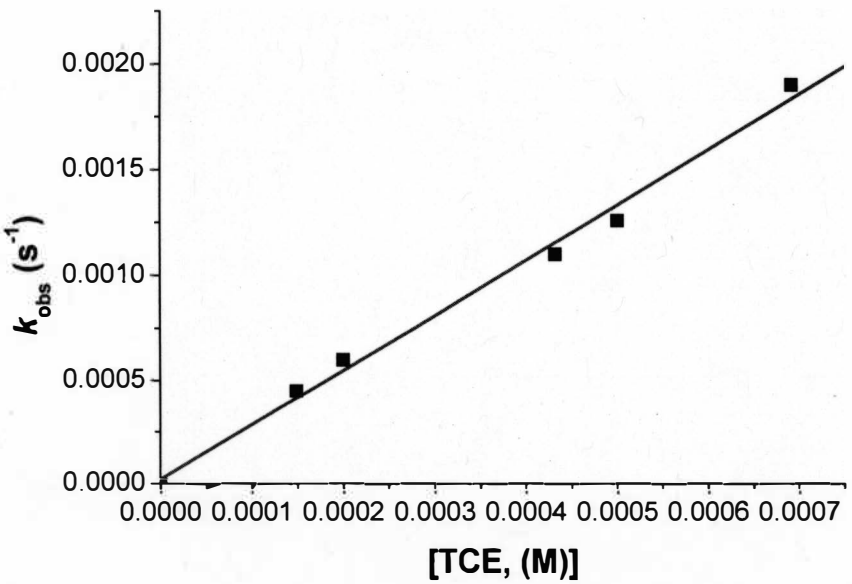

Figure 3.13 A linear fit plot of reduction rate constant (k) of TCE on $FMNH_2/TiO_2$ catalyst in aqueous solution as a function of k_{obs} vs. concentration of TCE

The generation of conduction band electrons resulted from anchoring FMN onto nanocrystalline TiO_2 thin film has shown reactivity towards TCE reduction in aqueous solution. We have shown that binding molecular catalysts FMN to TiO_2 surface enhances their reactivity towards organohalide (RX) pollutants as compared to fluid or aqueous

solution only. This ability to tune the reactivity of surface bound molecular catalysts by changing the solvents has significant effects on the reactivity towards specific RX pollutants. In aqueous solution, there is a fast charge-recombination of electron-hole pair as compared to methanol solvent. As a result, there is no charge accumulation of TiO_2 in the conduction band as shown by the lack of diversion in the UV-visible absorbance spectrum of TiO_2.

Comparison of the reduction rate constant of $FMNH_2$ in methanol solvent *vs.* $FMNH_2$ anchored on TiO_2 nanoparticles further confirmed that the reduction rate of TCE is enhanced when $FMNH_2$ is anchored to the surface relative to when it is in fluid solution. The reactivity of this $FMNH_2/TiO_2$ hybrid catalyst in aqueous solutions promises a wide range of research in green chemistry catalysis by avoiding organic solvent and at the same time promoting specific chemical transformations. Furthermore, reactivity towards TCE was initiated in the *dark* redox reaction, resulting in the elimination of toxic byproducts.

3.3.5 Reactivity of $FMNH_2/TiO_2(e^-_{CB})$ towards Trichloroethylene in Methanol Solvent

Irradiation of TiO_2 with energy equal to or greater than its band gap energy (Eg = 3.2 eV) resulted in a electron-hole charge separation [14]. Methanol is a well known OH· scavenger with a homogeneous bimolecular rate constant of 9.2×10^8 mol dm^{-3} s^{-1} [28]. In methanol solvent, this electron-hole charge separation is longer-lived compared to in aqueous solution because it undergoes longer charge separated state. As a result, the

accumulation of conduction band electrons is more noticeable in methanol solvent as observed in the dark-blue coloration of the TiO_2 thin film.

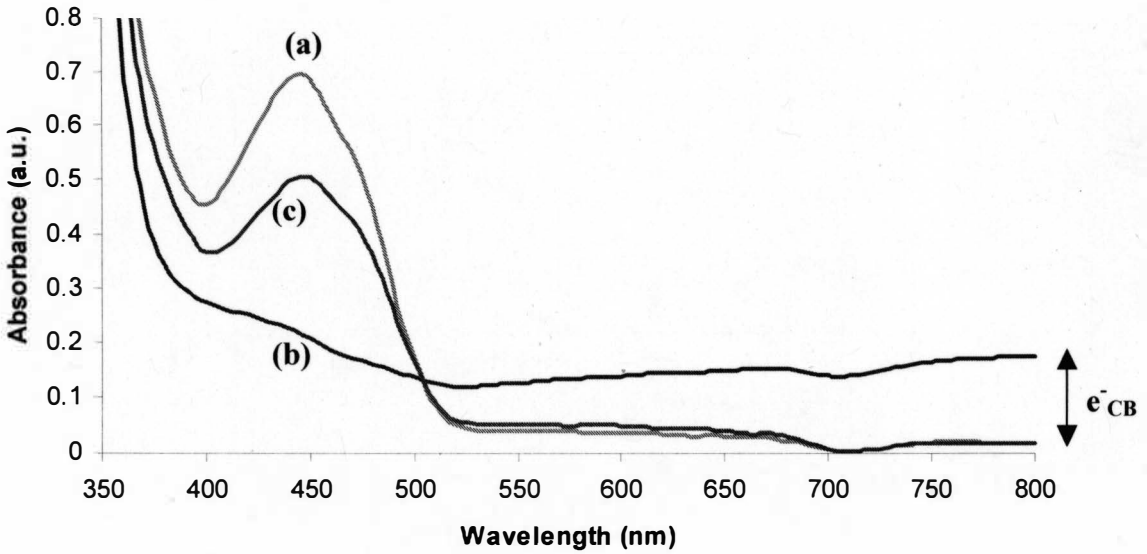

Figure 3.14 UV-visible absorbance spectra of $FMNH_2/TiO_2(e^-_{CB})$ in methanol solvent (a) before irradiation, (b) after irradiation and (c) after addition of TCE in the *dark*

Following band gap irradiation, FMN was reduced to $FMNH_2$, followed by electron being trapped and accumulated in the conduction band, resulting in $FMNH_2/TiO_2(e^-_{CB})$. This is shown by the 400 - NIR region [10, 20, 22] as shown in Figure 3.14. Addition of TCE to the $FMNH_2/TiO_2(e^-_{CB})$ in the *dark* was found to generate the initial FMN/TiO_2 absorption spectrum.

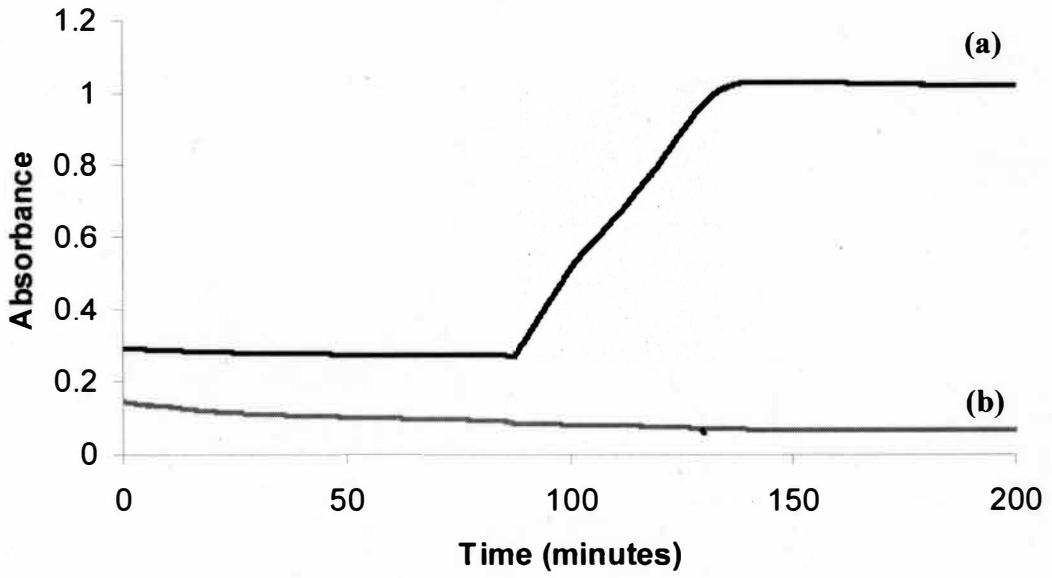

Figure 3.15 Time resolved absorption changes of $FMNH_2/TiO_2(e^-_{CB})$ monitored at (a) 445 nm and at (b) 700 nm following the addition of TCE in the *dark*

Pseudo-first order steady-state kinetics of TCE reacting with $FMNH_2/TiO_2(e^-_{CB})$ is shown in Figure 3.15. The measurement at 700 nm represents the $TiO_2(e^-_{CB})$, whereas the measurement at 445 nm represents the FMN absorbance spectrum. Injection of saturated TCE in water resulted in the reduction of TCE and oxidation of FMN to $FMNH_2$. From the time resolved absorption spectra, it was shown that $FMNH_2$ oxidation to FMN follows an interesting pattern: steady-state absorbance kinetics, followed by the steep increase in absorbance which then leveled off in steady-state absorbance kinetics. This is observed for all the kinetic experiments, possibly due to the presence of multiple electrons accumulating in the conduction band. Valence band holes irreversibly oxidize

methanol to formaldehyde under these conditions, which allows the $TiO_2(e^-_{CB})$ concentration to increase with steady-state irradiation [29].

Pseudo-first order kinetic rate constant, k_{obs} were obtained by fitting the data to equation 3.1. The slope of the graph generated from this plot is the corresponding reduction rate constant (k). In this particular system, the reduction rate constant of TCE is calculated to be 67.9 M^{-1} s^{-1}.

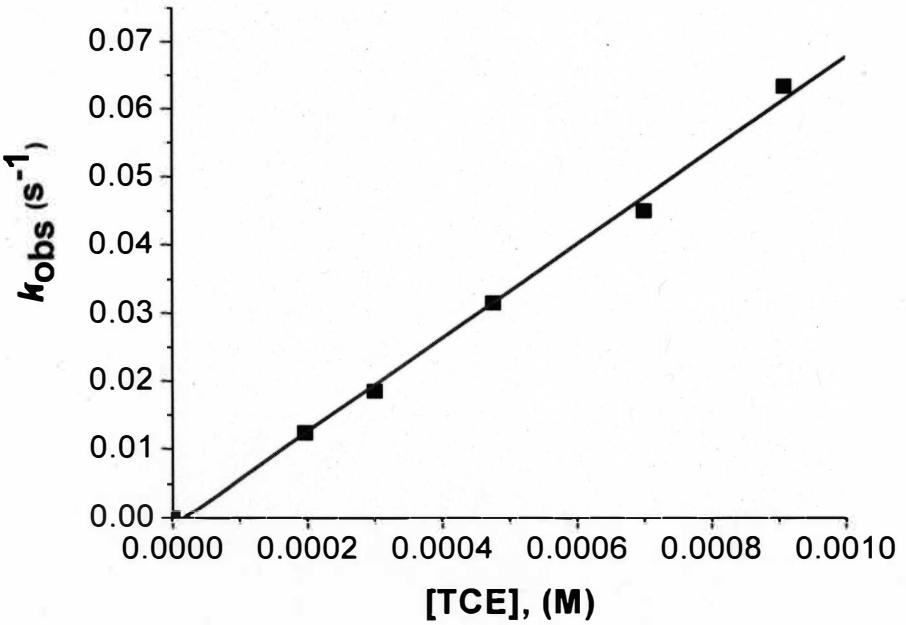

Figure 3.16 Plot of reduction rate constant (k) of TCE on $FMNH_2/TiO_2(e^-_{CB})$ hybrid catalyst in aqueous solution as a function of k_{obs} *vs.* concentration of TCE

The results further confirmed that in the presence of multiple electrons, the reduction rate of TCE degradation is two orders of magnitude higher compared The results further confirmed that in the presence of multiple electrons, the reduction rate of TCE degradation is two orders of magnitude higher compared just FMNH2 in solution, or $FMNH_2$ anchored to TiO_2 alone (with no $TiO_2(e^-_{CB})$).

Table 3.1 shows a comparison of the reduction rate constant values under each of the conditions. The results demonstrate that anchoring FMN onto the TiO_2 surface enhances its reactivity toward TCE. It was calculated that the TCE reduction rate constant by $FMNH_2/TiO_2(e^-_{CB})$ is one order of magnitude higher compared to $FMNH_2/TiO_2$. This result can be explained by the presence of multiple electrons. In methanol, it was estimated that about 600 electrons can be stored in an individual TiO_2 nanoparticle while in water the value is about a factor of 3 less [12]. The multi-electron transfer process allows the catalytic dehalogenation process to occur more efficiently and under mild conditions.

Table 3.1 Pseudo-first-order Rate constants (k) of TCE reduction by $FMNH_2$, TiO_2 (e^-), $FMNH_2/TiO_2$ in water, and $FMNH_2/TiO_2(e^-_{CB})$ in methanol*

RX	TiO_2(e-) k (M^{-1} s^{-1})	$FMNH_2$ k (M^{-1} s^{-1})	$FMNH_2/TiO_2$ in H_2O k (M^{-1} s^{-1})	$FMNH_2/TiO_{2(}e^-_{CB)}$ in CH_3OH k (M^{-1} s^{-1})
TCE	No Rxn	0.5	2.6	67.9

*Data collected at room temperature at multiple error trial

3.3.6 Reduction Potentials for Semiconductor-Supported Molecular Catalyst

Formal reduction potentials ($E^{0'}$) for FMN were measured in fluid solution and when anchored onto TiO_2 surfaces. Cyclic voltammetry was used to measure formal potentials in $TBAPF_6/CH_3CN/H_2O$ electrolyte. The FMN redox chemistry showed equivalent anodic and cathodic peak currents, ipa/ipc ~ 1 (Nernestian behavior). The cyclic voltammogram of FMN in $TBAPF_6/CH_3CN/H_2O$ electrolyte is shown in Figure 3.16. The $FMN/FMNH_2$ formal potentials were measured to be –570 mV vs. Ag/AgCl (3 M KCl) in 0.1 M $TBAPF_6/CH_3CN/H_2O$ electrolyte.

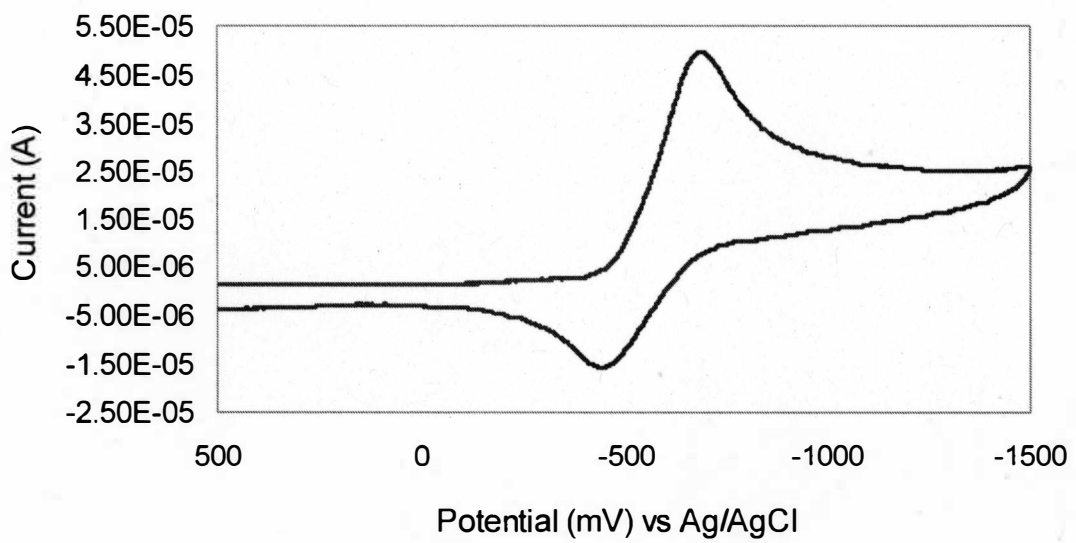

Figure 3.17 Cyclic voltammogram of FMN in 0.1 M $TBAPF_6/CH_3CN/H_2O$ electrolyte. Woking electrode is glassy carbon, reference electrode is Ag/AgCl, and the counter electrode is Pt wire. The scan rate is 100 mV/s

Measuring accurate FMN reduction potentials upon surface binding to TiO_2 using cyclic voltammetry was not feasible due to the strong oxidation of TiO_2 which overlaps with the FMN oxidation. An alternative route to measuring the formal reduction potential of FMN when anchored to the TiO_2 surface is by spectroelectrochemistry. The experimental set-up is shown in Figure 3.18, while the data obtained is shown in Figure 3.19. Spectroelectrochemical techniques have been developed which take advantage of the facts that nanostructured metal oxide films may be deposited on conducting glass supports to yield transparent electrodes and that electrons present in these electrodes have an optical spectroscopy characteristic of their local environment. The formal reduction potentials correspond to the equilibrium potentials where the concentration of reduced and oxidized compounds was equal.

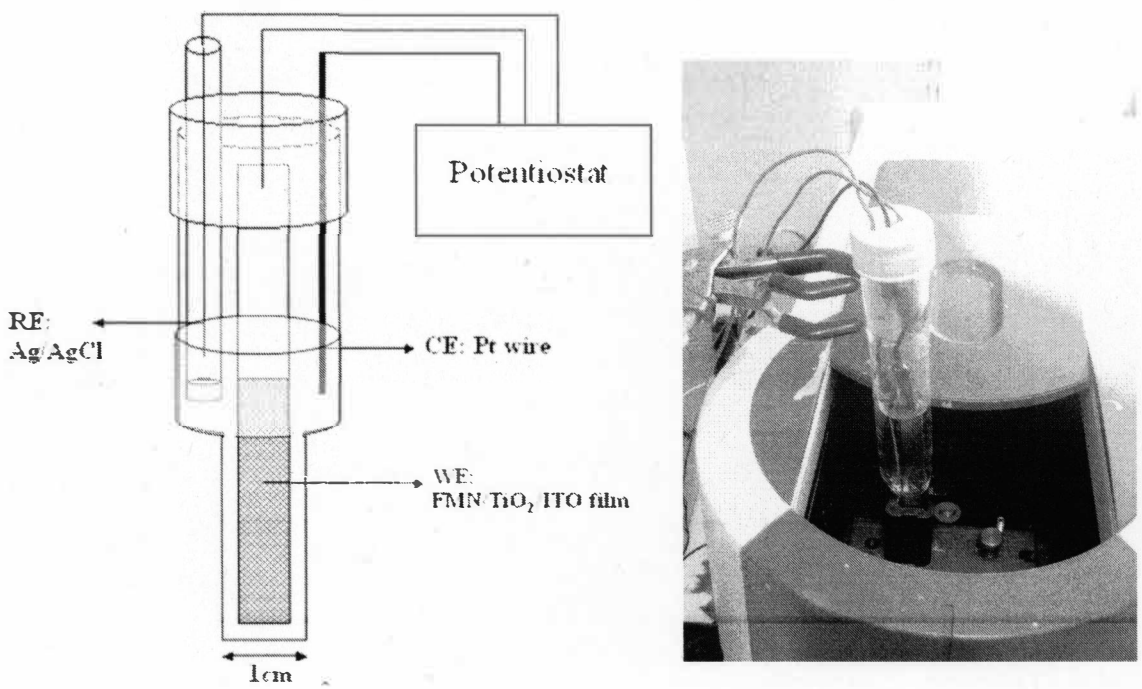

Figure 3.18 Left: Schematic representation of spectroelectrochemical cell. Right: Setup on the UV-visible absorbance spectrophotometer. Aligator clips were used to connect the electrodes

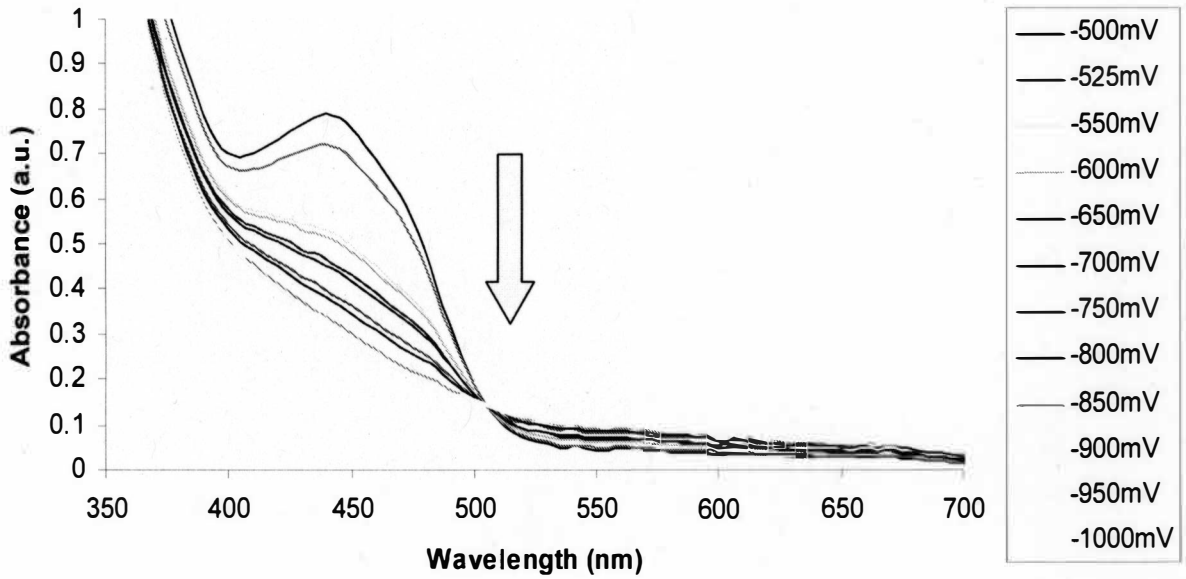

Figure 3.19 Representative spectroelectrochemical data of molecular catalyst FMN bound to TiO_2. FMN was reduced to $FMNH_2$ in $CH_3CN/TBAPF_6$ electrolyte upon applying negative potential. The potential applied were measured against Ag/AgCl (3 M KCl)

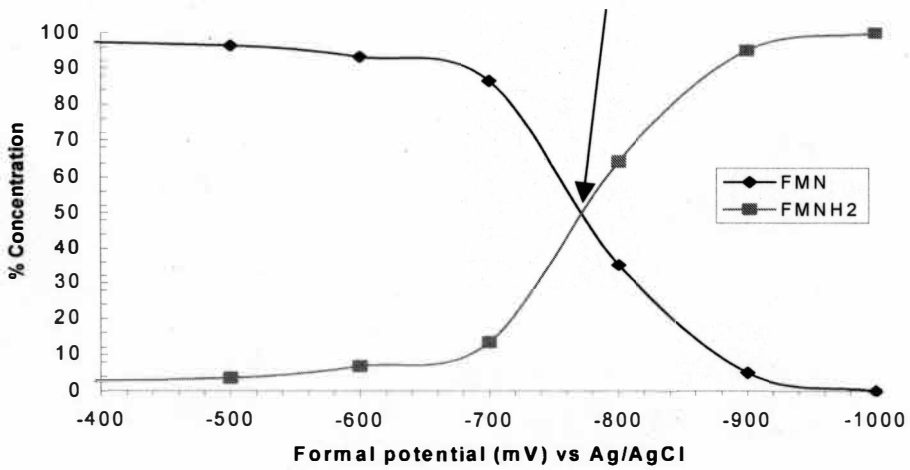

Figure 3.20 Plot of $FMN/FMNH_2$ concentrations vs. applied potential. The arrow line indicates the formal potential $E^{0'}$ of the system

The results of the spectroelectrochemical measurements show that surface binding has a profound effect on the formal potentials and RX reactivity of the catalysts. The formal potential of FMN bound to TiO_2 was calculated to be –775 mV vs. Ag/AgCl (3 M KCl), whereas the formal potential of FMN alone -570 mV vs. Ag/AgCl (3 M KCl). A significant shift in the formal reduction potential of FMN was observed upon surface binding, such that FMN bound to TiO_2 was always a stronger reductant than FMN in fluid solution. This observation explains the enhanced organohalide reactivity on the TiO_2 surface compare to in fluid solution. It is also noted that with a more negative applied bias, or band gap illumination, it is possible to mediate the reduction with TiO_2 conduction band electrons. The *dark* redox chemistry is initiated with FMN bound to the surface, and extends to the TiO_2 by intermolecular electron hopping. Complete oxidation of all the catalysts thus requires that there are no electronically isolated regions of the film and that a pathway for hopping to each catalyst is present [12].

3.3.7 TCE Degradation Product in $FMNH_2/TiO_2(e^-_{CB})$ in Methanol Solvent

The reduction of TCE in the $FMNH_2/TiO_2(e^-_{CB})$ were monitored and analyzed periodically with GC/MS. Figure 3.21 shows a plot of the decrease in TCE concentration (mol/L) over time as it reacts at room temperature.

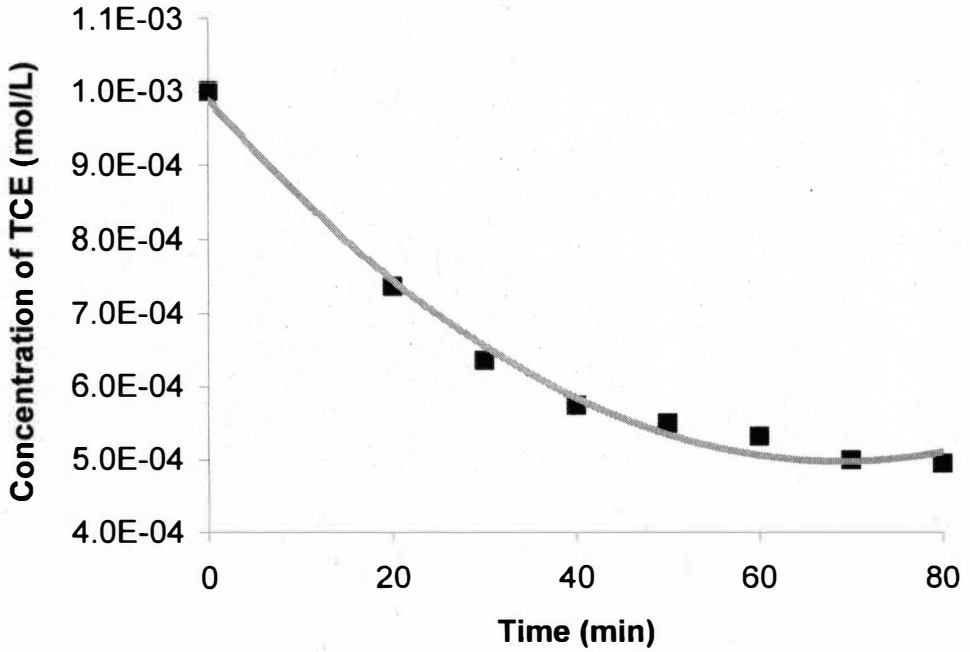

Figure 3.21 Plot of [TCE] vs. time during the degradation by $FMNH_2/TiO_2(e^-_{CB})$ at room temperature

It was observed that the TCE concentration decreases significantly over a period of 80 minutes. GC/MS analysis of the solution after decrease in the concentration of TCE showed no formation of any products. This prompted head-space analysis, which showed the presence of the gas – ethylene. This data is in agreement with two-electron transfer catalysts that have been used for TCE degradation. This result proves that the $FMNH_2/TiO_2(e^-_{CB})$ is an effective catalyst for TCE environmental remediation since no *cis*-dichloroethylene nor vinyl chloride are formed as reduction products. To prove this result, $FMNH_2/TiO_2(e^-_{CB})$ reoxidation to FMN/TiO_2 were analyzed spectroscopically by UV-visible as shown in Figure 3.22. Control experiments performed without TCE addition in the *dark* showed no reactivity.

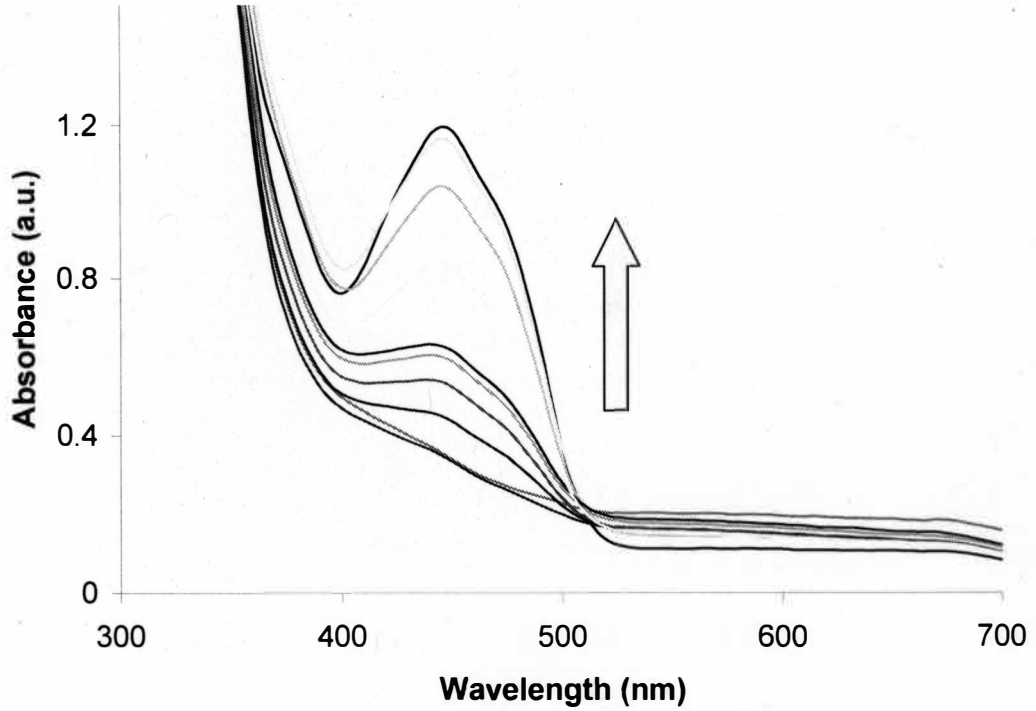

Figure 3.22 UV-visible absorbance spectra of $FMNH_2/TiO_2(e^-_{CB})$ re-oxidation following TCE addition in the *dark*. A spectrum was collected according to TCE withdrawal for GC/MS analysis

3.4 Conclusions

Reduced flavin mononucleotide (FMN) bound to mesoporous nanocrystalline (anatase) TiO_2 thin film as $FMNH_2/TiO_2$ showed enhanced reactivity toward TCE relative to $FMNH_2$ in fluid solution. The rate constant for the reduction of TCE in $FMNH_2/TiO_2(e^-_{CB})$ was calculated to be one order of magnitude higher than $FMNH_2/TiO_2$, and two orders of magnitude higher than $FMNH_2$ in fluid solution alone. The enhanced in the case of $FNMH_2/TiO_2$ relative to $FMNH_2$ alone can be attributed to the shifts in the FMN reduction potentials upon surface binding. Spectroelectrochemical

measurements of the formal reduction potential of $FMNH_2$ on the TiO_2 surface was found to be -775 mV vs. Ag/AgCl, which in comparison to the formal reduction potential of $FMNH_2$ in solution alone (–570 mV vs. Ag/AgCl) is shifted by 205 mV more negative. Such shifts make $FMNH_2$ bound to TiO_2 stronger reducing agents. In the case of $FMNH_2/TiO_2(e^-_{CB})$, the enhanced reactivity relative to either $FMNH_2$ alone or $FMNH_2/TiO_2$, is attributed to the presence of multiple electrons generated by the combination of both $FMNH_2$ and TiO_2 conduction band electrons ($TiO_2(e^-_{CB})$).

The studies shown indicate that the binding of molecular catalysts to semiconductor surfaces offers the following advantages: (1) enhance the reactivity due to shifts in formal reduction potentials, (2) ability to easily analyze reaction products due to the system being heterogeneous, (3) the presence of multiple electrons which favors enhanced reactions under mild conditions. Such systems can be further exploited for future environmental remediation applications.

3.5 References

1. Anpo, M., Utilization of TiO_2 photocatalysts in green chemistry. Pure and Applied Chemistry, **2000**. *72(7):* p. 1265-1270.

2. Espenson, J.H., Petovsky, O., Huston, P., and Saudt, S., Organometallic catalysis in Aqueous Solution: Oxygen Transfer to Bromide. Journal of the American Chemical Society, **1994**. *116*: p. 2869-2877.

3. Orth, W.S. and R.W. Gillham, Dechlorination of trichloroethene in aqueous solution using Fe0. Environmental Science and Technology, **1996**. *30*: p. 66-71.

4. Schrick, B., Blough, J.L., Jones, D., and Mallouk, T.E., Hydrodechlorination of Trichloroethylene to Hydrocarbons Using Bimetallic Nickel-Iron Nanoparticles. Chemistry of Materials, **2002**. *14*: p. 5140-5147.

5. Clufford, J.N., Palomares, E., Nazeeruddin, M., Thampi, R., Gratzel, M and Durant, J., Multistep Electron Transfer Processes on Dye Co-sensitized Nanocrystalline TiO_2 Films. Journal of the American Chemical Society, **2004**. *126.* p.5670-5671

6. Hoffmann, M.R., Martin, S.T., Choi, W., and Bahnemann, D.W, Environmental Applications of Semiconductor Photocatalysis. Chemical Reviews, **1995**. *95*: p. 69-96.

7. Choi, W. and M.R. Hoffmann, Kinetics and Mechanism of CCl4 Photoreductive Degradation of TiO2: The role of Trichloromethyl Radical and Dichlorocarbene. Journal of Physical Chemistry, **1996**. *100:* p. 2161-2169.

8. Mayer, I., Nakamura, M., Toma, H.E., and Ariki, K., Multielectronic redox and electroanalytic supramolecular films based on a tetraruthenated iron porphyrin. Electrochimica Acta, **2006**. *2006*(52): p. 263-271.

9. Tributsch, H., Multi-electron transfer catalysis for energy conversion based on abundant transition metals. Electrochimica Acta, **2007**. *52*: p. 2302-2316.

10. R.Stromberg, J., Wnuk, J.D., Pinlac, R.F., and Meyer, G.J., Multielectron Transfer at Heme-Functionalized Nanocrystalline TiO_2: Reductive Dechlorination of DDT and CCl_4 Forms Stable Carbene Compounds. Nano Letters, **2006**. *6(6):* p. 1284-1286.

11. Obare, S.O., T. Ito, M. Balfour and G.J. Meyer, Ferrous Hemin Oxidation by Organic Halides at Nanocrystalline TiO_2 Interfacess. Nano Letters, **2003.** *3(8):* p. 1151-1153.

12. Obare, S.O., T. Ito, and G.J. Meyer, Controlling Reduction Potentials of Semiconductor-Supported Molecular Catalysts for Environmental Remediation of Organohalide Pollutants. Environmental Science and Technology, **2005**. *39*: p. 6266-6272.

13. Canevali, C., Morazzoni, F., Scotti, R., Giusti, M., Testino, A., Musinu, A., and Cannas, C., Nanocrystalline TiO_2 with Enhanced Photoinduced Charge Separation as Catalyst for the Phenol Degradation. International Journal of Photoenergy, **2006**. *90809*: p. 1-6.

14. Chen, X. and S.S. Mao, Titanium Dioxide Nanomaterials: Synthesis, Properties, Modifications and Applications. Chemical Reviews, **2007**.107(7): p. 2891-2959

15. Prairie, M.R., Evans, L.R., Stange, B.M., and Martinez, S.L., An investigation of TiO_2 Photocatalysis for the Treatment of Water Contaminated with Metals and Organic Chemicals. Environmental Science and Technology, **1993**. *27:* p. 1776-1782.

16. Alberici, R.M., Mendes, A.M., Jardim, W.F., and Eberlin, M.E.., Mass Spectrometry On-Line Monitoring and MS2 Product Characterization of TiO_2/UV Photocatalytic Degradation of Chlorinated Volatile Organic Compounds. Journal of American Society of Mass Spectrometry, **1998**. *9*: p. 1321-1327.

17. Choi, W., Hong, S.J., Chang, Y.S., and Cho, Y., Photocatalytic degradation of polychlorinated dibenzo-p-dioxins on TiO_2 film under UV or solar light irradiation. Environmental Science and Technology, **2000**. *34*: p. 4810-4815.

18. Okuya, K.N. and S. Kaneko, Porous TiO_2 thin films synthesized by a spray deposition (SPD) technique and their application to dye-sensitized solar cells. Solar Energy Mater. Solar Cells, **2002**. *70*: p. 425-435.

19. Galoppini, E., Linkers for anchoring sensitizers to semiconductor nanoparticles. Coordination Chemistry Reviews, **2004**. *248*: p. 1283.

20. Redmond, G., D. Fitzmaurice, and M. Graetzel, Effect of Surface Chelation on the Energy of an Intraband Surface State of a Nanocrystalline TiO_2 Film. Journal of Physical Chemistry, **1993**. *97*: p. 6951-6954.

21. Heimer, T.A., D'Arcangelis, S.T., Farzad, F., Stipkala, J.M., and Meyer, G.J., An Acetylacetonate-Based Semiconductor-Sensitizer Linkage. Inorganic Chemistry, **1996**. *35*: p. 5319-.

22. Howe, R.F. and M.J. Gratzel, EPR observation of trapper electrons in colloidal titanium dioxide. Journal of Physical Chemistry, **1987**. *91(14):* p. 4495-4499.

23. Highfield, J.G. and M. Gratzel, Discovery of Reversible Photochromism in Titanium Dioxide Using Photoacoustic Spectroscopy. Implications for the Investigation of Light-Induced Charge Separation and Surface Redox Processes in Titanium Dioxide. **1988.** *92*: p. 464-467.

24. Boschloo, G. and D. Fitzmaurice, Electron Accumulation in Nanostructured TiO_2 (anatase) Electrodes. Journal of Physical Chemistry B, **1999**. *103:* p. 7860-7868.

25. Lyon, L.A. and J.T. Hupp, Energetics of the Nanocrystalline Titanium Dioxide/Aqueos Solution Interfaces: Approximate Conduction Band Edge Variations between H_0 = -10 and H- = +26. Journal of Physical Chemistry B., **1999**. *103*: p. 4623-4628.

26. Guangquan, L., Linsbigler., A.L and J.T. Yates, Photolysis on TiO_2 Surface. Chemical Reviews, **1995**. *95*: p. 735-758.

27. Pelizzetti, N., and Serpone, N, Photocatalysis: Fundamentals and Applications. **1989**, New York: Wiley-Interscience.

28. Mandelbaum, P.A., Regazonni, A.E., Blesa, M.A, and Bilmes, S.A., Photo-electro-oxidation of alcohols on titanium dioxide thin film electrodes. Journal of Physical Chemistry B., **1999**. *103*: p. 5505-5511

29. Tamaki, Y., Furube, A., Murai, M., Hara, K., Katoh, R, and Tachiya, M., Direct Observation of Reactive Trapped Holes in TiO_2 Undergoing Photocatalytic Oxidation of Adsorbed Alcohols: Evaluation of the Reaction Rates and Yields. Journal of the American Chemical Society, **2005**. *128*: p. 416-417.

30. Roberts, A.L., Burris, D.R., Delcomyn, C.A., and Smith, M.H.., Reductive Dechlorination of Tetrachloroethylene and Trichloroethylene Catalyzed by Vitamin B_{12} in Homogeneous and Heterogeneous Systems. Environmental Science and Technology, **1996**. *30*: p. 3047-3052.

31. Bachmann, J., Hodgkiss, J.M., Yong, E.R., and Nocera, D., Ground and Excited State Reactivity of Iron Porphyrinogens. Inorganic Chemistry, **2007**. *46*: p.607-609.

32. Barbe, C., Papageorgiou, N., and Gratzel, M., Morphology and Adsorbate Dependence of Ionic Transport in Dye Sensitized Mesoporous TiO_2 Films. Journal of Physical Chemistry B., **1998**. 102: p. 4156-4164